TITLE PAGE

Manuscript Title

Identification of novel plasma proteomic biomarkers of Dupuytren Disease

Authors

Blake Hummer[1]

Paola Sebastiani[2,3] ORCID 0000-0001-6419-1545

Anastasia Leshchyk[4] ORCID 0000-0002-2830-6701

Anastasia Gurinovich[2,3] ORCID 0000-0001-9808-9397

Cecilie Bager[5] ORCID 0000-0003-2430-9777

Morten Karsdal[5] ORCID 0000-0001-5026-8740

Signe Nielsen[5] ORCID 0000-0002-4612-1014

Charles Eaton*[1] ORCID 0000-0002-8186-3611

Affiliations

1. Dupuytren Research Group, West Palm Beach, FL
2. Institute for Clinical Research and Health Policy Studies, Tufts Medical Center, Boston, MA
3. Department of Medicine, Tufts University, Boston, MA

4. Department of Medicine, Computational Biomedicine Section, Chobanian & Avedisian School of Medicine, Boston University, Boston, MA

5. Nordic Bioscience, Herlev, Denmark

* Corresponding Author Charles Eaton MD, Dupuytren Research Group 1850 Forest Hill Blvd STE 201, West Palm Beach, FL 33406 1.561.429.8279 c.eaton.md@dupuytrens.org

KEYWORDS

Dupuytren contracture

Fibrosis

Biomarker discovery

Collagen

Proteomic

Identification of novel plasma proteomic biomarkers of Dupuytren Disease

ABSTRACT

Dupuytren Disease (DD) is a chronic progressive disease that can cause disabling hand deformities. The most common treatments have high rates of complications and early recurrence. Dupuytren lacks a staging biomarker profile to develop preventive therapeutics to improve long-term outcomes. This multi-omic study aimed to create a DD blood proteomic biomarker profile by comparing DD plasma to a healthy control group. We measured circulating collagen metabolism peptides and found normal Collagen I synthesis but impaired Collagen I degradation in DD. We measured 6995 serum protein aptamers and identified 68 proteins with statistically significant differences from the control group. We developed two Diagnostic Proteomic Risk Scores (DPRS) based on hypothesis-free and hypothesis-based analyses. In independent data, our hypothesis-free and the hypothesis-based DPRS distinguished Dupuytren from control subjects with 76.5% and 70.6% accuracy, respectively. Our hypothesis-based DPRS also distinguished DD subjects with different disease progression rates based on subject age at the time of their first corrective procedure (p=0.0018). This pilot study is the first to provide evidence that Collagen I accumulation in DD is due to impaired degradation rather than increased collagen synthesis. It also describes novel DPRS that have potential use as diagnostic and staging biomarker panels for Dupuytren disease.

Identification of novel plasma proteomic biomarkers of Dupuytren Disease

Introduction

Dupuytren disease (DD) is a progressive fibrotic condition that often results in finger deformities called Dupuytren contracture (DC). DD affects an estimated 10 million Americans. DC is associated with loss of productivity, higher healthcare costs, and a greater prevalence of benign diseases[1].

The greatest need in DD care is preventing DC progression and recurrence. As with other fibrotic diseases, developing preventive treatments requires a biomarker profile for staging and measuring therapeutic response. The authors have not found published reports with statistically significant evidence of preventing DC recurrence or a biomarker tool to develop such treatments. This pilot study aimed to develop preliminary data on a diagnostic blood biomarker profile of DD.

DC is a common outcome of DD. Of those diagnosed with DD at age 65, one in four men and one in eight women will require at least one corrective procedure over their lifetime[2]. Current treatments are palliative, often with partial or temporary improvement[3]. Surgery for DC has a greater risk of major complications than other common elective hand operations[4-7], and recurrent DC is the most common diagnosis leading to elective finger amputation[8].

Genetic factors account for about 80% of the risk of developing DD[9]. Family history, age, and gender have strong associations. A genetic risk score (GRS) based on 11 SNPs correlates with DD diagnosis[10], and a weighted GRS based on 26 SNPs correlates with post-procedure recurrence[11].

DD affects the palm skin, subcutaneous tissues, and fascia[12]. Early disease is cellular, with fibroblasts, myofibroblasts, and perivascular clusters of myofibroblasts, pericytes, and mononuclear immune cells[13]. Early changes include local variations of immune[13], hematopoietic, and mesenchymal cell markers[12], cytokines, signaling factors[14], and

extracellular matrix components[15,16]. Progression transforms tissues into nearly acellular densely packed collagen.

Physical changes are the basis for DD diagnosis, staging, and treatment, but physical findings don't predict progression[17]. There are no standard noninvasive tests of DD biological activity. Biopsy is problematic because it can trigger disease activity and progression. In addition, DD-related tissue findings do not always correlate with blood measurements[18-20], and DD tissue gene expression does not correlate with local protein levels[21]. Blood remains the most promising source for a disease activity profile.

We conducted a discovery study to compare levels of circulating proteins and peptides in subjects with DD versus controls using ELISA, aptamer, and mass spectrometry methods. We found statistically significant differences in disease versus control cohorts in independent analyses of peptides and proteins. We also found statistically significant differences in protein aptamers in DD subjects with different rates of clinical progression of untreated disease.

RESULTS

Assessment of Collagen Metabolism in DD.

Collagen synthesis and degradation processes release protein fragments specific to the process, collagen type, and enzyme involved. The ratio of synthesis to degradation-related fragments correlates with net accumulation or loss of that collagen type. We evaluated plasma collagen synthesis and degradation markers using the competitive ELISA method (Nordic Biosciences; Herlev, Denmark) and calculated collagen synthesis-to-degradation ratios[22].

We measured markers of types I, II, III, IV, V, VI, VII, and IX collagen metabolism in blood from a cohort of healthy controls (n = 14) and subjects with DD (n = 13). We found significantly low levels of markers of Collagen I degradation C1M (Figure 1A, p = 0.004), Collagen V synthesis Pro-C5 (Figure 1B, p = 0.046), and Collagen VII synthesis Pro-C7 (Figure 1C, p = 0.048) in the

DD cohort compared to the control group. The remaining collagen biomarkers did not show significant differences between the disease and control groups (Table 1).

We calculated collagen synthesis-to-degradation ratios for collagen types I, II, III, IV, and V. The Collagen I synthesis to degradation ratio Pro-C1/C1M was significantly greater in the DD cohort compared to the control group (Figure 1D, $p = 0.024$). The remaining ratios were not significant (Col II, III, IV, VI) or could not be calculated because the degradation marker was either unavailable (Col V, IX) or not detectable in both disease and control cohorts (Col VII).

Assessment of Differentially Expressed Blood Proteins in DD.

We performed two orthogonal unbiased proteomic methods, the aptamer-based SomaScan (SomaLogic; Boulder, CO) and liquid chromatography-tandem mass spectrometry (LC-MS/MS) (MacCoss Lab, University of Washington, WA, USA).

We used sixty-nine samples for SomaScan testing after quality control (36 DD and 33 controls). These represent 42 subjects, 27 of whom had second samples obtained six to fourteen months after the first (Supplementary Fig. S1 online). The SomaLogic panel measures 6995 protein binding sites applying to 5444 proteins.

Hypothesis-free approach

The 6995 aptamer measurements identified 54 proteins with statistically significant differences between DD and control groups, with 24 overexpressed and 30 underexpressed after adjusting for multiple comparisons (Supplementary Table S1 online). Figure 2 is a heatmap of these 54 protein expressions.

We performed pathway analysis of these 54 proteins to identify network relationships using STRING[23]. We found significant protein-protein interactions (PPI) in 29, with multiple enriched categories (Figure 3C, p-value = 4.55E-04). Supplementary Table S2 online summarizes

categories of enriched gene groups, and Supplementary Fig. S2 online provides a visual cross-reference of functional categories and individual genes. The dominant categories were coagulation and complement cascades, the extracellular matrix, enzyme inhibition, cell membrane structures, phosphorylation, and signaling pathways.

Hypothesis-free Diagnostic Proteomic Risk Score (DPRS)

Using the SomaScan results, we aimed to develop a hypothesis-free indicator of DD diagnosis with a calculated Diagnostic Proteomic Risk Score (DPRS) to estimate an individual's disease risk based on plasma protein abundance.

We developed a hypothesis-free DPRS estimation based on two of the 54 proteins. These proteins, OSCAR (overexpressed) and SPART (underexpressed), had a low relative correlation (Pearson's correlation coefficient = -0.19) (Table 2), suggesting minimal interaction. Using this hypothesis-free DPRS as a diagnostic measure for DD achieved an accuracy of 79% in the training set (AUC 0.8) and 76.5% in the test set (Figure 3A), indicating a predictive value for discriminating between disease and control. Figure 3B shows a boxplot of control and DD DPRS. The DPRS calculated for controls and DD significantly differed by the Wilcoxon test (p-value = 2.5E-06).

Hypothesis-based approach

We also conducted a hypothesis-based approach with 328 relevant proteins identified from a literature search and available on the SomaLogic platform (Supplementary Table S3 online). Twenty-three proteins in this subset had statistically significant differences between DD and control, with nine overexpressed and fourteen underexpressed after adjusting for multiple comparisons (Supplementary Table S4 online).

We performed PPI networks and enrichment analysis on these 23 proteins using STRING. We found significantly enriched PPI in 21 proteins with multiple enriched categories (Figure 4C, p-

value = 1.35e-07). We found more enrichment categories and greater significance in the hypothesis-based than the hypothesis-free analysis, which may reflect a higher-yield group, selection bias, or both. Supplementary Table S5 online lists enriched gene categories, and Supplementary Fig. S3 online provides a visual cross-reference between functional categories and individual genes.

Hypothesis-based Diagnostic Proteomic Risk Score

We developed a hypothesis-based DPRS using 11 of 23 DE proteins identified in the hypothesis-based analysis. Six genes were underexpressed (*SMAD1, SH3BP2, LCN2, USP8, CSNK1G2, SERPINH1*) and five overexpressed (*CSMD1, POSTN, ACAN, AOC3, DDR2*). Six proteins were present in hypothesis-based and hypothesis-free DPRS analyses (Table 3). Our hypothesis-based DPRS achieved a training accuracy of 78.85% (AUC 0.9) and a test accuracy of 70.59% in distinguishing Dupuytren from control cohorts (Figure 4A). Figure 4B shows that DPRS distributions of Control and DD groups differ significantly (Wilcoxon test (p-value = 2.2E-09).

Evaluation of DRPS for Prognosis

We explored the potential of each DPRS to profile DD prognosis using the rate of contracture progression as an index of biological severity. We segregated our DD samples into subjects younger (11 specimens) or older (16 specimens) than 50 at the time of their first DC procedure. We excluded subjects younger than 50 from this analysis. A one-way ANOVA analysis unveiled a statistically significant variance in the means of hypothesis-driven generated DPRS across groups with different rates of pretreatment contracture progression (Supplementary Fig. S4 online, p-value = 0.0018). Conversely, we found no associations in the DPRS generated through the hypothesis-free approach.

Mass Spectrometry

Identification of novel plasma proteomic biomarkers of Dupuytren Disease

The LC-MS dataset contained 48 samples: 27 DD and 21 controls. This assay identified 561 peptides. No peptides had statistically significant differences in abundance across groups (FDR > 0.25).

Mass-Spectrometry-SomaScan Concordance

To further validate our Somascan findings, we evaluated the MS results for concordance. Of the 54 significant proteins from the SomaScan data analysis, six were present in the Mass Spectrometry findings: AOC3, POSTN, SERPINC1, TF, PCSK9, and KNG1. We ran the same analyses on these six proteins using Mass Spectrometry data. AOC3, POSTN, and SERPINC1 had adjusted p-values (FDR) <0.25 in both Mass Spec and SomaLogic analyses (Table 4).

DISCUSSION

This study aimed to discover candidate biomarkers that correlate with the diagnosis of DD as the first step toward a diagnostic DD blood test.

Dynamic biomarker panels are essential to developing preventive therapeutics for chronic diseases like DD. The relevance of this study is that DD lacks such biomarkers. Blood is the most promising unexplored source of proteomic biomarkers for trend analysis.

There are no broad surveys of circulating proteins in DD. In addition, blood findings may not parallel tissue findings because of rapid degradation, intracellular or membrane-bound locations, post-translational variants, protein binding, and other mechanisms. Because of this, new and diverse discovery research is necessary to profile DD-associated blood protein biomarkers.

There are two common biomarker discovery strategies: hypothesis-free and hypothesis-based. The hypothesis-free approach (unbiased or non-hypothesis-based) screens many markers and is the standard in systems biology and discovery research. The hypothesis-based strategy evaluates selected markers based on published information and is the most common model of DD research. We used both methods in this study.

Collagen accumulation is the hallmark of DD. DD-affected tissues have unique proportions of collagen types I[24], III[25], IV[16], and V[24]. The most prominent tissue changes in the progression from preclinical to end-stage disease are increases in total Collagen I and the proportion of Collagen III[24].

Our hypothesis-based approach compared collagen synthesis and degradation markers in DD versus control groups. Collagen turnover releases circulating peptides unique to the synthesis and degradation of each collagen type. In the absence of disease, synthesis and degradation markers are tightly coupled. Plasma synthesis to degradation marker ratios can indicate net collagen gain, loss, or homeostasis[22]. We used ELISA to measure plasma levels of sixteen collagen metabolism markers involving eight collagen types. We summarize our findings in Table 1.

The DD cohort had normal Collagen I synthesis marker Pro-C1 levels but statistically significant decreases in Collagen I degradation marker C1M (Figure 1A), resulting in an elevated synthesis-to-degradation marker ratio of DD compared to controls (Figure 1D). These findings suggest DD collagen accumulation follows impaired Collagen I degradation rather than excess collagen synthesis. Both degradation-resistant collagen variants and reduced collagenase activity may contribute to reduced collagen degradation.

Dupuytren collagen has two features that increase resistance to enzymatic degradation. Typical Collagen I fibrils are heterotrimers of two Collagen I α1 strands and one collagen I α2 strand.

DD-affected tissues have an increased proportion of α1 (I) homotrimer Collagen I[26]. DD collagen also has more crosslinks stabilized by hydroxylation and glycosylation[27]. Both homotrimer Collagen I[28] and glycosylation-stabilized crosslinks[29] increase resistance to enzymatic cleavage.

DD-related dysregulation of collagenases and their inhibitors impair collagen degradation by several mechanisms. TIMP1 (Tissue Inhibitor of Metalloproteinase 1) inhibits multiple MMPs and is elevated in the circulation of DD patients[18]. MMP1, MMP8, MMP13, and MMP14 gene polymorphisms are associated with Dupuytren disease[30,31], including MMP14 partial loss-of-function variants[31]. MMP14 is necessary for MMP2 activation, and both enzymes facilitate myofibroblast contraction[32].

Two clinical findings support a relationship between impaired collagen degradation and DD. The first is the rapid onset of DD with metalloproteinase inhibitor treatment[33]. The second is abnormally slow matrix remodeling in DD. Enzymatic cleavage of collagen fibrils is necessary for matrix shortening[34], and impaired cleavage would slow this process. Slow matrix remodeling could explain why DD-related tissue shortening progresses more slowly than wound healing despite similar biology and why DD surgery has an increased risk of delayed wound healing[35].

The hallmark of fibrotic diseases is collagen accumulation. Increased collagen synthesis contributes to collagen accumulation in pulmonary fibrosis[36], liver fibrosis[37], primary biliary cirrhosis[38], renal fibrosis[39], and cardiovascular disease[40]. Our finding of normal levels of circulating Collagen I synthesis biomarkers in DD suggests that the mechanism of collagen accumulation in DD is not due to the increased collagen synthesis associated with these diseases. Although often used interchangeably with increased collagen synthesis, neither collagen accumulation nor upregulated collagen gene expression is de facto evidence of increased collagen synthesis. Cell culture studies show increased *COL1A1* and *COL1A2* mRNA

expression in DD-derived fibroblasts[21,41], but these RNA findings are not associated with increased collagen I protein production[21]. Our finding of normal Collagen I synthesis and impaired degradation informs future research because DD drug development has focused on reducing collagen synthesis rather than increasing degradation[42].

Collagen II markers were normal. We evaluated Collagen II markers because of the correlation between DD and psoriasis[43] and the finding of abnormal Collagen II in psoriasis[44]. We found no significant differences between groups in Collagen II synthesis marker PRO-C2_HP and degradation marker C2M_HP or their ratios. The CALC2 synthesis marker was undetectable in both cohorts, preventing the calculation of CALC2 synthesis-to-degradation ratios.

Collagen III synthesis markers were normal, consistent with a prior report of normal circulating Collagen III synthesis marker amino-terminal propeptide of type III procollagen (PIIINP) in DD subjects[45]. Given the accumulation of Collagen III in DD, we expected to find elevated Collagen III synthesis to degradation marker ratios. Instead, we found normal Collagen III synthesis to degradation ratios. This finding may reflect that other proteases also degrade Collagen III, and we did not measure all potential collagen degradation fragments. To investigate further, we assayed a different Col III degradation marker CTX-III_HP on the remaining aliquots. Only 17 (10 DD, 7 Controls) of the initial 27 (13 DD, 14 Controls) leftover aliquots had sufficient residual volumes for this assay. Although this small subgroup's CTX-III violin plot appearance suggested reduced degradation in DD compared to controls (Supplementary Fig. S5 online), this difference was not statistically significant.

We found significantly lower Collagen V synthesis marker Pro-C5 levels in the DD cohort than controls (Figure 1B). This finding is unexplained. An increased percentage of Collagen V is reported in DD tissues[24], suggesting a high Collagen V synthesis to degradation ratio.

However, we could not calculate this ratio because a Collagen V degradation marker was unavailable.

The DD cohort also had significantly lower Collagen VII synthesis marker Pro-C7 than controls (Figure 1C). We could not calculate Collagen VII synthesis to degradation ratios because Collagen VII degradation markers were undetectable in both cohorts. Although there are no reports of Collagen VII in DD, its role in matrix mechanobiology and elevated tissue levels in systemic sclerosis[46] makes it a potential marker for collagen metabolism abnormalities in DD.

We found no significant differences in the measurements of the remaining collagen markers. We measured Collagen IV markers because Collagen IV is increased in DD tissues[16]. We assayed Collagen VI markers and ratios because prior pathway analysis suggests a role for Collagen VI in DD and other fibrotic diseases[47]. We selected Collagen IX markers based on unpublished data suggesting a role in DD. None of these markers or ratios showed significant differences between disease and control cohorts.

Separate from the Nordic collagen fragment analysis, we analyzed whole proteins with the SomaLogic aptamer-based platform. The SomaLogic panel measures 6995 protein binding sites associated with 5444 proteins. Supplementary Table S6 online lists genes and gene aliases of proteins mentioned in this manuscript.

SomaLogic hypothesis-free analysis identified 54 distinct proteins with significantly different plasma levels than controls. Twenty-three proteins had increased levels, and 29 had lower DD levels than controls (Supplementary Table S1 online). Our findings are consistent with existing literature.

The body of DD research publications mentions only seven of these 54 differentially expressed proteins: Aggrecan (*ACAN*), Amine Oxidase Copper Containing 3 (*AOC3*), Caspase-3 (*CASP3*), Periostin (*POSTN*), SMAD Family Member 1 (*SMAD1*), Spartin (*SPART*), and Ubiquitin

carboxyl-terminal hydrolase 8 (*USP8*). Our differential expression findings concur with reports of *ACAN*[48], *AOC3*[13], and *POSTN*[49] overexpression in tissue and *SMAD1*[50], *SPART*[51], and *USP8*[51] underexpression in cell culture. CASP3 levels were low in our findings but are upregulated in a report of transcriptomic profiling[48]. This finding is unexplained. *ACAN* is also near the variant rs6496519 associated with DD[52]. Supplementary Table S1 online summarizes the relevance of these 54 genes to DD.

We constructed PPI networks and enrichment analysis of these 54 plasma proteins, revealing significantly enriched protein-protein interactions in 32 with multiple enriched protein groups and categories (Supplementary Fig. S2 online, Supplementary Table S2 online). These categories aligned with known Dupuytren cellular biology. Abnormalities in the KEGG category has04610 (complement and coagulation cascades) were consistent with DD pathway meta-analysis findings[53]. Complement fragments induce adhesion molecules that act on endothelial cells, consistent with DD-related perivascular clusters of immune cells and small vessel occlusion[13]. Complement fragments also activate mast cells that release TNF, a known DD pathway component[54], and histamine, a driver of itching, which is common in early-stage DD[55]. Cell membrane and extracellular matrix signaling receptor binding of growth factors, cytokines, and other signaling factors play pivotal roles in DD pathobiology[14]. Protein phosphorylation processes are consistent with increased phosphorylated STAT1, STAT3, SMAD2, SMAD3, and ERK1/2 in DD tissues[50,56,57]. The enriched Reactome HSA-162582 (Signal Transduction) pathway is noteworthy, as it includes signaling by TGF-Beta, WNT, and NOTCH, all prominent in DD biology[58].

We based our hypothesis-free DPRS on high levels of Osteoclast-associated immunoglobulin-like receptor (*OSCAR*) and low levels of Spartin (*SPART*) (Table 2). Our finding of elevated OSCAR levels is interesting because Collagen I is an OSCAR ligand. OSCAR also stimulates T-cells to release TNF[59], a component of DD biology[54]. Our finding of decreased *SPART* levels is

consistent with low *SPART* expression in DD fibroblasts[51]. SPART is also associated with Epidermal Growth Factor Receptor (EGFR) degradation and transport to the cell membrane[60], consistent with increased ratios of intracellular to cell membrane EGFR levels found in DD[61].

Separate from the hypothesis-free analysis, we conducted a hypothesis-based analysis using a subset of the SomaLogic proteins selected from an independent literature review (Supplementary Table S3 online). We found 23 proteins in this subset with significantly different plasma levels than controls. Nine proteins had higher, and fourteen had lower levels in DD than controls. Nine proteins were present in both hypothesis-free and hypothesis-based groups. Our findings are consistent with existing literature. Supplementary Table S4 online summarizes the potential relationships of these proteins and parent genes to DD.

With our hypothesis-free analysis, we performed a STRING PPI analysis of the hypothesis-based findings to identify network relationships of the 23 proteins. We found significantly enriched protein-protein interactions in 21 with multiple enriched categories (p-value = 1.35e-07, Supplementary Table S5 online). This analysis implicated enrichment categories in addition to those from the hypothesis-free analysis. Myofibroblast differentiation, proliferation, motility, WNT signaling, and interleukin pathways are unsurprising, given their known roles in DD biology[10,20]. Cancer pathway associations are also unsurprising, given the correlations of DC with carcinomas and sarcomas[62,63]. Infection-related pathways were unexpected and exclusively involved viral and parasitic infection categories. This finding might be due to a hidden variable of tissue repair biology, which overlaps interleukin-driven parasitic immune defense biology and interleukin-related DD biology.

This hypothesis-based analysis provided data to generate a second Diagnostic Proteomic Risk Score (DPRS) calculated on eleven proteins (Table 3). Figure 4A shows the AUC-ROC of this panel (AUC = 0.9), and Figure 4B shows the DPRS based on this panel distinguishing DD from control cohorts.

We evaluated the potential of each DPRS for staging. Recurrence after a procedure is the benchmark of Dupuytren's biological severity. Traditionally, surgeons use clinical factors such as early age of onset, affected family members, and disease locations other than the palms to predict post-procedure recurrence. However, the study's inclusion criteria included these factors, so we could not use them to subset our Dupuytren cohort. Instead, we used age at the time of the first DC procedure. Small studies suggest that recurrence is more common in patients younger at their first DC procedure[64,65]. We evaluated the ability of each DPRS to distinguish Dupuytren subjects who had their first corrective procedure before age 50 versus those having their first correction at age 50 or older. The hypothesis-based DPRS distinguished DD subjects requiring their first DC procedure before age 50 from those having their first procedure after age 50 (p=0.0018), suggesting potential use as a staging and predictive tool.

Although Mass Spectrometry did not reveal statistically significant differences in abundance across cohorts, there was statistically significant concordance between Mass Spec and SomaScan findings. The Mass Spec data contained 6 of the 54 proteins with statistically significant differences between disease and control cohorts using the hypothesis-free SomaScan data analysis: Amine Oxidase Copper Containing 3 *AOC3*, Periostin *POSTN*, Serpin Family C Member 1 *SERPINC1*, Transferrin *TF*, Proprotein Convertase Subtilisin/Kexin Type 9 *PCSK9*, and Kininogen 1 *KNG1*). Table 4 compares the results of the SomaLogic and Mass Spectrometry data analysis. A pathway analysis of these six proteins identified two highly significant Reactome categories (Supplementary Table S7 online). In addition to protein phosphorylation noted above, Reactome HSA-381426 involving Insulin-like Growth Factor *IGF* and Insulin-like Growth Factor Binding Proteins *IGFBP*s is relevant because of the role of IGF-II and IGFBP-6 in regulating Dupuytren fibroblast proliferation and contractility[66].

This study has limitations. Statistical disadvantages were the small number of samples in all assays and the large number of aptamers in the SomaScan assay. Although our findings align

with current research on Dupuytren proteomics, there are differences. Elevated serum TIMP1[18] and TNF[20] have been reported in DD, but we found no statistically significant DE between disease and control groups. This discrepancy may reflect that Somalogic assays target specific protein conformations, whereas ELISA measures all conformations.

SUMMARY

In summary, we used ELISA, aptamer, and mass spectrometry assays to identify differential plasma proteomic signatures between DD and control cohorts. We found significant DD-related proteomic abnormalities in both collagen metabolism peptide fragments and whole proteins in circulation. This study is the first to have evidence suggesting that net collagen accumulation in DD derives from normal collagen synthesis and impaired collagen degradation, challenging the model of excess collagen synthesis and distinguishing DD from other organ fibroses. Normalizing impaired collagen degradation should be a lead target for therapeutic drug development. We independently analyzed proteins from the same cohorts. Our hypothesis-free analysis of 5444 proteins revealed 54 with statistically significant differences between DD and control cohorts. Our independent hypothesis-based analysis of 328 proteins selected from the literature review identified 23 with statistically significant differences. We developed two Dupuytren Diagnostic Proteomic Risk Scores separately based on hypothesis-free and hypothesis-driven analyses. We used pathway analyses to identify DD protein-protein network enrichments, confirming known DD interactions and revealing previously unreported DD pathway categories. Finally, we showed our hypothesis-based DPRS correlated with the subject's age at the time of the first DD procedure, an index of biological severity. These findings suggest that a validated hypothesis-based DPRS could guide management and develop DD therapeutics.

We recommend a larger study to validate our Collagen I, III, V, and VII metabolite findings. We also recommend a validating study of 68 unique proteins identified in the protein aptamer

analysis (54 in the hypothesis-free analysis and 23 in the hypothesis-based analysis, with 9 in both groups). Testing only the subset of the 68 most pertinent proteins would increase the statistical power. Individual ELISA assays would be cost-prohibitive. An alternative would be a custom multiplex panel for the 13 proteins in our two DPRS[14] to validate our DPRS and the correlation of our hypothesis-based DPRS on age at the first DD procedure. Our findings strongly support the need to fund and conduct more extensive validating studies of circulating collagen metabolites and proteins in DD. This biomarker research is fundamental to developing DD diagnostic tests to diagnose, stage, and inform research to develop therapeutic drugs for DD.

METHODS

Sex as a biological variable

Our study involved male and female subjects. Sex was not considered a biological variable.

Subjects

We selected disease cohort subjects from the International Dupuytren Database (IDDB), an online patient-reported registry developed by the Dupuytren Research Group (DRG) in collaboration with the National Databank of Rheumatic Diseases (NDB). Control subjects were enrolled by word of mouth and from the NDB database (https://dupuytrens.org/enroll-in-the-iddb-2/). All subjects in the IDDB met the entry criteria and signed an Informed Consent Form.

Entry Criteria

The DD cohort met criteria based on clinical evidence of DD with strong traditional predictors of recurrent deformity after a corrective procedure: age of disease onset younger than 50; two or more first-degree relatives with DD; current DD nodules; three or more separate locations of DD or two palm locations and Ledderhose disease (a related disorder). Control cohort subjects

were healthy individuals with no clinical evidence of DD, no personal history of DD or Ledderhose disease, and no family history of DD.

We confirmed study eligibility by requiring candidates to upload recent images of each hand's palmar and dorsal sides. The Principal Investigator/ senior author confirmed entry criteria and reviewed images to confirm clinical evidence of active DD in the disease cohort and the lack of these findings in the control cohort.

Blood Sample Collection

The study used a mobile phlebotomy service to collect blood specimens (Phlebotek Solutions Corporation, Fort Lauderdale, FL). Once confirmed that the subject met all study entry criteria, they were contacted by DRG and later by Phlebotek to schedule their blood draw. The phlebotomist visited the subjects in their homes and collected two tubes of blood. The last 16 blood draws included a third 2.5ml PAXgene tube collection for additional genomic testing.

Processing of the EDTA tubes for proteomic testing was standardized. Immediately following collection, blood samples were centrifuged for 15 minutes at 2000 g to generate plasma. The plasma was harvested from the top of the container and pooled before aliquoting into storage cryotubes. The last 500 uL of plasma was discarded to avoid contamination with platelets. Samples were immediately packaged for shipping on dry ice.

Number of subjects

One hundred subjects were planned (50 DD/50 Control). Blood collection launched just as the COVID pandemic began (i.e., February 2020). Due to COVID-related issues, we amended the protocol to enroll 50 subjects. Forty-seven subjects were enrolled;46 subjects had samples drawn. One sample was disqualified due to failed shipping refrigeration. Samples from the remaining 45 subjects (25 DD, 20 Control) had mass-spectrometry (Bioproximity, Manassas, VA). Twenty-seven subjects (13 DD, 14 control) had second blood samples drawn six to 14

months after their first draw for mass-spectrometry testing by a second lab (MacCoss Lab, Seattle, WA). Additional proteomic testing was conducted on remaining aliquots; 1) n= 27 redrawn samples had ELISA tests for collagen metabolites (Nordic Bioscience, Herlev, DK) 2) n= 72 from both initial and redraw specimens had Aptamer-based testing (SomaLogic, Boulder, CO). Supplementary Fig. S1 online outlines the distribution of samples and laboratories.

Blinding

All subjects were assigned and identified as participant numbers. Investigators were blinded to the sample group allocation. All samples remained blinded throughout the processing and data collection in the laboratories.

Assays

Nordic Bioscience Collagen Biomarker Assay

Circulating collagen synthesis and degradation markers were measured using proprietary assays[22]. Synthesis biomarkers included collagens I (PRO-C1), II (PRO-C2), III (PRO-C3), IV (PRO-C4), V (PRO-C5), VI (PRO-C6), VII (PRO-C7), and IX (PRO-C9). Circulating degradation markers were measured for collagens I (C1M), II (CALC2, C2M), III (C3M, CTX-III), IV (C4M), VI (C6M), and VII (C7M). All biomarkers were assessed by competitive ELISAs and validated to measure in human plasma samples. The inter- and intra-assay coefficients of variation were >15% and 10%, respectively, for all assays.

Mass Spectrometry

A novel untargeted proteomics assay using a large-scale liquid chromatography-tandem mass spectrometry (LC-MS/MS) approach called data-independent acquisition (DIA) was used to collect proteomic data. Each sample (10 µl plasma), following tryptic digestion, was diluted

50:50 by the addition of 4% sodium dodecyl sulfate (SDS) buffer to a final concentration of ~2% SDS. Approximately 200 µg of protein was added to 96 well-plates, and the remainder of the sample preparation was performed using the single-pot, solid-phase enhanced sample preparation for proteomics methodology (SP3) [67,68]. The entire process of protein capture, reduction and alkylation, protein cleanup, digestion, and peptide cleanup was performed using a KingFisher magnetic bead robot[68]. Peptides were reconstituted in HPLC starting aqueous buffer (5% acetonitrile and 0.1% formic acid) with analysis performed on the high-resolution quadrupole-orbitrap hybrid mass spectrometer (Exploris 480, Orbitrap Fusion Lumos, or Orbitrap Fusion Eclipse).

Data was acquired in a single, 2-hour LC-MS/MS run (90 min HPLC gradient) on a Thermo Quadrupole-Orbitrap mass spectrometer. Crucially, the DIA method comprehensively samples all peptides between 400 and 1000 m/z using a repeated cycle of 75 MS/MS scans with an 8 m/z-wide isolation width. Using a multiplexing scheme based on staggering the isolation window in alternating cycles of MS/MS scans, the precursor selectivity of the resulting data is 4 m/z after computational demultiplexing[69]. From the resulting data, fragment ion chromatograms were extracted for any peptide precursor between 400 and 1000 m/z. To determine which peptides are confidently detected in each acquisition, the software tool EncyclopeDIA[70] was used to query the data using a reference chromatogram library generated from a prior analysis of the tissue. Chromatogram-based relative-quantitation was then performed for each peptide detected. All measurements are made relative to a common reference. In the case of plasma, a common reference is a pooled standard from 400 age matched samples from subjects who are both healthy and span the phenotypes being studied processed in each sample batch. Within each 96-well plate, one copy of the common reference standard is placed in each row for a total of 8 copies per plate[71]. Before quantification, it is confirmed that peptides are stable during the

time scale of the data collection, have a suitable linear response, and have suitable intra and inter-data precision.

SomaScan Assay

SomaLogic, Inc. (Boulder, CO, USA) performed proteomic analysis of the plasma samples using a SomaScan platform that quantifies the presence of 6995 human proteins (secreted proteins, extracellular domains, and intracellular proteins). These proteins are found in diverse biological groups such as receptors, kinases, cytokines, proteolytic enzymes and inhibitors, growth factors, protease inhibitors, hormones, and structural proteins[72]. Most of these proteins involve pathways relating to signal transduction, stress response, immune processes, phosphorylation, proteolysis, cell adhesion, cell differentiation, and intracellular transport[73].

Proteins were measured using the Slow Off-Rate Modified Aptamer (SOMAmer)-based capture array that uses chemically modified single-stranded DNA sequences capable of uniquely recognizing individual proteins via one or more binding sites. SOMAmers transform a protein signal to a nucleotide signal that is quantified using relative fluorescence on microarrays. Each SOMAmer array underwent validation for specificity, upper and lower limits of detection, and both intra- and interassay variability. Plasma dilutions (0.005%, 0.05%, and 20%) were applied to capture low-, medium- and high-abundance proteins. Positive and negative controls were also positioned on the array to confirm if the experimental procedure was performed correctly.

After the hybridization step, the microarrays were washed and scanned using a laser scanner that excites the fluorescence of the fluorochrome used in the labeling step. The amount of the emitted signal is directly proportional to the dye on the microarray. The scanner measures this quantity and creates a digital image map the position of each signal based on the location of its origin. Image analysis software generates a text file from this map describing pixel intensity of

the spot and the background. This information was processed, and a final value was generated that summarized the level of each detectable protein on the microarray.

Quality control analysis of the sample and SOMAmer levels involved SOMAmer control arrays on the microarray and calibration samples. Hybridization controls measured the sample-by-sample variation in hybridization, while the median signal over all SOMAmer arrays measured the technical variability. The SomaScan measures were reported as relative fluorescence units (RFU) in a summary ADAT file.

Protein-protein interaction network and pathway analysis

STRING (12.0) is a web tool that provides and illustrates protein-protein interaction and networks[23]. STRING integrates different types of evidence from public databases, including genomic context, high-throughput, and biochemical interaction experiments, known protein complexes, computational predictions, and text-mining from scientific literature. Given a list of gene names, STRING will construct protein-protein interaction networks where each gene is considered as a node, with edges representing the predicted functional associations.

Networks were generated using the whole genome as the statistical background, and interaction sources included text mining, experiments, databases, co-expression, neighborhood, gene fusions, and co-occurrence. Interaction scores were created by combining the probabilities from all evidence channels and corrected for the probability of randomly observing an interaction. All nodes and interactions were computed with a required medium confidence interaction score (0.400) and an FDR<=0.05.

Analysis and statistics

Nordic collagen data turnover rates were calculated by performing ratios of the propeptide over the mature peptide (e.g., PRO-C1/ C1M). This ratio is an estimate of the formation/degradation

of each collagen type and can be interpreted as a net gain of collagen/loss of collagen remodeling[22]. All comparisons were done using Student's T-test.

A series of quality control and data cleaning steps were performed on the SomaLogic proteomics data. All non-human proteins were excluded from the analyses. Samples that did not pass the default normalization acceptance criteria for all row scale factors were removed. All aptamers that did not pass the default quality control criteria across all plates/sets were filtered out. The data had no missing values, and the protein values were log-transformed. No further normalization was performed.

We identified differentially expressed aptamers using linear regression of each log-transformed protein as the outcome and disease status as the main predictor. We adjusted each analysis by age and sex. We analyzed all repeated measurements of each individual and employed generalized estimating equations to account for technical and biological variability using the gee package in R. Due to the high number of aptamers tested in the SomaScan assay (6995), we were at a statistical testing disadvantage regarding multiple corrections. Therefore, we calculated adjusted p-values using Benjamini Hochberg methods. Our SomaLogic analyses only report proteins with statistically significant differences from control at an FDR-adjusted p-value < 0.25.

For the MS protein data, all zeroes were replaced with NAs across samples, and protein values were log-transformed. The MS dataset was subset based on proteins that overlapped with the signature proteins associated with DD previously identified using the SomaScan proteomics data. We used a generalized estimation equation model to account for the repeated blood draws, adjusted by age and gender.

Proteomic Risk Score

To prepare the data for the Diagnostic Proteomic Risk Score (DPRS) calculation, we first removed all highly correlated proteins (Pearson correlation > 0.8). 3369 out of 6995 aptamers were highly correlated and were excluded from the DPRS calculation. The DPRS calculation contained the following two steps. First, we fit a logistic regression for each protein with disease status (i.e., case or control) as the outcome variable adjusted by age and gender. We used a generalized estimation equation model for repeated measurements of two independent blood draws. We included the same subject's repeated measurements and used the generalized estimation equations model with the gee R package[74] to estimate the regression coefficients. Next, the DPRS was computed using summary statistics from each regression model. Only the proteins with statistically significant differences from control at an FDR-adjusted p-value < 0.25 were included in the score calculation. The DPRS was calculated by summing the beta estimated effect for all significant proteins, each multiplied by normalized protein abundance and divided by its standard error. Finally, we fit a logistic regression to examine the association of the computed DPRS with DD onset. We split the dataset into training (75%) and testing sets utilizing the caret R package for a leave-one-out cross-validation approach for model fitting and assessment (25%) sets[75]. We used R version 4.2.1 for all analyses.

Study Approval

The Institutional Review Board Ascension Via Christi Hospitals Wichita, Inc. approved this study and the associated informed consent form. The written informed consent was signed and received before subject participation. This written informed consent included a description of the use of the photographs/ images to be reviewed for study entry. The records of these signed informed consents have been retained. All samples remained blinded throughout the processing and data collection in the laboratories. All methods were performed in accordance with relevant guidelines, regulations, and the Declaration of Helsinki.

References

1 Macaulay, D., Ivanova, J., Birnbaum, H., Sorg, R. & Skodny, P. Direct and indirect costs associated with Dupuytren's contracture. *J Med Econ* **15**, 664-671, doi:10.3111/13696998.2012.670678 (2012).

2 Broekstra, D. C., Kuo, R. Y. L., Burn, E., Prieto-Alhambra, D. & Furniss, D. Dupuytren Disease: Prevalence, Incidence, and Lifetime Risk of Surgical Intervention. A Population-Based Cohort Analysis. *Plast Reconstr Surg* **151**, 581-591, doi:10.1097/PRS.0000000000009919 (2023).

3 Mendelaar, N. H. A. *et al.* Outcome of Recurrent Surgery in Dupuytren's Disease: Comparison with Initial Treatment. *Plast Reconstr Surg* **144**, 828e-835e, doi:10.1097/PRS.0000000000006150 (2019).

4 Goodman, A. D., Gil, J. A., Starr, A. M., Akelman, E. & Weiss, A.-P. C. Incidence of Serious Complications in Hand Surgery: A 10-Year Review. *The Journal of Hand Surgery* **41**, S27-S28, doi:10.1016/j.jhsa.2016.07.047 (2016).

5 Schindelar, L., McEntee, R., D'Amore, T., Beredjiklian, P. & Lutsky, K. Unplanned Return to the Operating Room in Upper-Extremity Surgery: Incidence and Reason for Return. *J Hand Surg Am* **46**, 715 e711-715 e712, doi:10.1016/j.jhsa.2021.01.019 (2021).

6 Denkler, K. Surgical complications associated with fasciectomy for dupuytren's disease: a 20-year review of the English literature. *Eplasty* **Jan 27**, e15 (2010).

7 Alser, O. *et al.* Serious complications and risk of re-operation after Dupuytren's disease surgery: a population-based cohort study of 121,488 patients in England. *Sci Rep* **10**, 16520, doi:10.1038/s41598-020-73595-y (2020).

8 Degreef, I. & De Smet, L. Dupuytren's disease: a predominant reason for elective finger amputation in adults. *Acta Chir Belg* **109**, 494-497, doi:10.1080/00015458.2009.11680467 (2009).

9 Larsen, S. *et al.* Genetic and environmental influences in Dupuytren's disease: a study of 30,330 Danish twin pairs. *J Hand Surg Eur Vol* **40**, 171-176, doi:10.1177/1753193414535720 (2015).

10 Dolmans, G. H. *et al.* Wnt signaling and Dupuytren's disease. *N Engl J Med* **365**, 307-317, doi:10.1056/NEJMoa1101029 (2011).

11 Riesmeijer, S. A. *et al.* A Weighted Genetic Risk Score Predicts Surgical Recurrence Independent of High-Risk Clinical Features in Dupuytren's Disease. *Plast Reconstr Surg* **143**, 512-518, doi:10.1097/PRS.0000000000005208 (2019).

12 Iqbal, S. A., Hindocha, S., Farhatullah, S., Paus, R. & Bayat, A. in *Dupuytren's Disease and Related Hyperproliferative Disorders* Ch. Chapter 21, 167-174 (2012).

13 Mayerl, C. *et al.* Characterisation of the inflammatory response in Dupuytren's disease. *J Plast Surg Hand Surg* **50**, 171-179, doi:10.3109/2000656X.2016.1140054 (2016).

14 Gonga-Cave, B. C., Pena Diaz, A. M. & O'Gorman, D. B. Biomimetic analyses of interactions between macrophages and palmar fascia myofibroblasts derived from Dupuytren's disease reveal distinct inflammatory cytokine responses. *Wound Repair Regen* **29**, 627-636, doi:10.1111/wrr.12928 (2021).

15 Halliday, N. L., Rayan, G. M., Zardi, L. & Tomasek, J. J. Distribution of ED-A and ED-B containing fibronectin isoforms in Dupuytren's disease. *J Hand Surg Am* **19**, 428-434, doi:10.1016/0363-5023(94)90057-4 (1994).

16 Magro, G., Fraggetta, F., Travali, S. & Lanzafame, S. Immunohistochemical expression and distribution of alpha2beta1, alpha6beta1, alpha5beta1 integrins and their extracellular ligands, type IV collagen, laminin and fibronectin in palmar fibromatosis. *Gen Diagn Pathol* **143**, 203-208 (1997).

17 Broekstra, D. C., Lanting, R., Werker, P. M. N. & van den Heuvel, E. R. Disease Course of Primary Dupuytren Disease: 5-Year Results of a Prospective Cohort Study. *Plast Reconstr Surg* **149**, 1371-1378, doi:10.1097/PRS.0000000000009115 (2022).

18 Ulrich, D., Hrynyschyn, K. & Pallua, N. Matrix metalloproteinases and tissue inhibitors of metalloproteinases in sera and tissue of patients with Dupuytren's disease. *Plast Reconstr Surg* **112**, 1279-1286, doi:10.1097/01.PRS.0000081462.40448.49 (2003).

19 Jupp, O. *et al.* in *Dupuytren Disease and Related Diseases - The Cutting Edge* Ch. Chapter 7, 55-61 (2017).

20 Wang, M. L. *et al.* Circulating inflammatory cytokines alter transcriptional activity within fibrotic tissue of Dupuytren's disease patients. *J Orthop Res*, doi:10.1002/jor.25059 (2021).

21 van Beuge, M. M., Ten Dam, E. J., Werker, P. M. & Bank, R. A. Matrix and cell phenotype differences in Dupuytren's disease. *Fibrogenesis Tissue Repair* **9**, 9, doi:10.1186/s13069-016-0046-0 (2016).

22 Karsdal MA *et al. Biochemistry of Collagens, Laminins and Elastin*. (Elsevier, 2019).

23 Szklarczyk, D. *et al.* The STRING database in 2023: protein-protein association networks and functional enrichment analyses for any sequenced genome of interest. *Nucleic Acids Res* **51**, D638-D646, doi:10.1093/nar/gkac1000 (2023).

24 Bailey, A. J. in *Dupuytren's Disease Biology and Treatment* Vol. 5 *Hand and Upper Limb Series* (eds RM McFarlane, DA McGrouther, & MH Flint) Ch. 6, (Churchill Livingstone, 1990).

25 Bailey, A. J., Sims, T. J., Gabbiani, G., Bazin, S. & LeLous, M. Collagen of Dupuytren's disease. *Clin Sci Mol Med* **53**, 499-502, doi:10.1042/cs0530499 (1977).

26 Williamson, K. *et al.* Active synthesis of type I collagen homotrimer in Dupuytren's fibrosis is unaffected by anti-TNF-α treatment. *bioRxiv preprint* doi:10.1101/2020.07.13.195107 (2023).

27 Bazin, S. *et al.* Biochemistry and histology of the connective tissue of Dupuytren's disease lesions. *Eur J Clin Invest* **10**, 9-16, doi:10.1111/j.1365-2362.1980.tb00003.x (1980).

28 Han, S. *et al.* Molecular mechanism of type I collagen homotrimer resistance to mammalian collagenases. *J Biol Chem* **285**, 22276-22281, doi:10.1074/jbc.M110.102079 (2010).

29 Snedeker, J. G. & Gautieri, A. The role of collagen crosslinks in ageing and diabetes - the good, the bad, and the ugly. *Muscles Ligaments Tendons J* **4**, 303-308 (2014).

30 Rodrigues, M. P. *et al.* MMP-1, MMP-8, and MMP-13 Gene Polymorphisms and Haplotype Is a Risk Factor for Dupuytren Contracture: A Case-Control Study. *Hand (N Y)*, 15589447241242818, doi:10.1177/15589447241242818 (2024).

31 Itoh, Y. *et al.* A common SNP risk variant MT1-MMP causative for Dupuytren's disease has a specific defect in collagenolytic activity. *Matrix Biol* **97**, 20-39, doi:10.1016/j.matbio.2021.02.003 (2021).

32 Wilkinson, J. M. *et al.* MMP-14 and MMP-2 are key metalloproteases in Dupuytren's disease fibroblast-mediated contraction. *Biochim Biophys Acta* **1822**, 897-905, doi:10.1016/j.bbadis.2012.02.001 (2012).

33 Krzeski, P. *et al.* Development of musculoskeletal toxicity without clear benefit after administration of PG-116800, a matrix metalloproteinase inhibitor, to patients with knee osteoarthritis: a randomized, 12-month, double-blind, placebo-controlled study. *Arthritis Res Ther* **9**, R109, doi:10.1186/ar2315 (2007).

34 Castella, L. F., Buscemi, L., Godbout, C., Meister, J. J. & Hinz, B. A new lock-step mechanism of matrix remodelling based on subcellular contractile events. *J Cell Sci* **123**, 1751-1760, doi:10.1242/jcs.066795 (2010).

35 Bismil, Q. *et al.* The development of one-stop wide-awake dupuytren's fasciectomy service: a retrospective review. *JRSM Short Rep* **3**, 48, doi:10.1258/shorts.2012.012050 (2012).

36 Organ, L. A. *et al.* Biomarkers of collagen synthesis predict progression in the PROFILE idiopathic pulmonary fibrosis cohort. *Respir Res* **20**, 148, doi:10.1186/s12931-019-1118-7 (2019).

37 Liu, T., Wang, X., Karsdal, M. A., Leeming, D. J. & Genovese, F. Molecular serum markers of liver fibrosis. *Biomark Insights* **7**, 105-117, doi:10.4137/BMI.S10009 (2012).

38 Vesterhus, M. *et al.* Comprehensive assessment of ECM turnover using serum biomarkers establishes PBC as a high-turnover autoimmune liver disease. *JHEP Rep* **3**, 100178, doi:10.1016/j.jhepr.2020.100178 (2021).

39 Han, D. C., Isono, M., Hoffman, B. B. & Ziyadeh, F. N. High glucose stimulates proliferation and collagen type I synthesis in renal cortical fibroblasts: mediation by autocrine activation of TGF-beta. *J Am Soc Nephrol* **10**, 1891-1899, doi:10.1681/ASN.V1091891 (1999).

40 Genovese, F. *et al.* Plasma levels of PRO-C3, a type III collagen synthesis marker, are associated with arterial stiffness and increased risk of cardiovascular death. *Atherosclerosis* **388**, 117420, doi:10.1016/j.atherosclerosis.2023.117420 (2024).

41 Satish, L., Gallo, P. H., Baratz, M. E., Johnson, S. & Kathju, S. Reversal of TGF-beta1 stimulation of alpha-smooth muscle actin and extracellular matrix components by cyclic AMP in Dupuytren's-derived fibroblasts. *BMC Musculoskelet Disord* **12**, 113, doi:10.1186/1471-2474-12-113 (2011).

42 Lambi, A. G., Popoff, S. N., Benhaim, P. & Barbe, M. F. Pharmacotherapies in Dupuytren Disease: Current and Novel Strategies. *J Hand Surg Am*, doi:10.1016/j.jhsa.2023.02.003 (2023).

43 Patel, M. *et al.* The prevalence of Dupuytren contractures in patients with psoriasis. *Clin Exp Dermatol* **39**, 894-899, doi:10.1111/ced.12424 (2014).

44 Holm Nielsen, S. *et al.* Differentiating patients with psoriasis from psoriatic arthritis using collagen biomarkers. *Clin Exp Rheumatol*, doi:10.55563/clinexprheumatol/jmt9jv (2022).

45 Gassier, N., Brenner, P., Berger, A. & Delbruck, A. in *Dupuytren's Disease Pathobiochemistry and Clinical Management* (eds A Berger, A Delbruck, P Brenner, & B Hinzmann) 94-98 (Springer-Verlag, 1994).

46 Sand, J. M. B. *et al.* Development of a Neo-Epitope Specific Assay for Serological Assessment of Type VII Collagen Turnover and Its Relevance in Fibroproliferative Disorders. *Assay Drug Dev Technol* **16**, 123-131, doi:10.1089/adt.2017.820 (2018).

47 Williams, L. M. *et al.* Identifying collagen VI as a target of fibrotic diseases regulated by CREBBP/EP300. *Proc Natl Acad Sci U S A* **117**, 20753-20763, doi:10.1073/pnas.2004281117 (2020).

48 Rehman, S. *et al.* Molecular phenotypic descriptors of Dupuytren's disease defined using informatics analysis of the transcriptome. *J Hand Surg Am* **33**, 359-372, doi:10.1016/j.jhsa.2007.11.010 (2008).

49 Vi, L. *et al.* Periostin differentially induces proliferation, contraction and apoptosis of primary Dupuytren's disease and adjacent palmar fascia cells. *Exp Cell Res* **315**, 3574-3586, doi:10.1016/j.yexcr.2009.07.015 (2009).

50 Krause, C., Kloen, P. & Ten Dijke, P. Elevated transforming growth factor beta and mitogen-activated protein kinase pathways mediate fibrotic traits of Dupuytren's disease fibroblasts. *Fibrogenesis Tissue Repair* **4**, 14, doi:10.1186/1755-1536-4-14 (2011).

51 Forrester, H. B. *et al.* Genome-wide analysis using exon arrays demonstrates an important role for expression of extracellular matrix, fibrotic control and tissue remodelling genes in Dupuytren's disease. *PLoS One* **8**, e59056, doi:10.1371/journal.pone.0059056 (2013).

52 Ng, M. *et al.* A Genome-wide Association Study of Dupuytren Disease Reveals 17 Additional Variants Implicated in Fibrosis. *Am J Hum Genet* **101**, 417-427, doi:10.1016/j.ajhg.2017.08.006 (2017).

53 Park, T. H., Kim, D., Lee, Y. S. & Kim, S. Y. A meta-analysis to identify novel diagnostic and therapeutic targets for Dupuytren's disease. *Wound Repair Regen* **28**, 202-210, doi:10.1111/wrr.12774 (2020).

54 Verjee, L. S. *et al.* Unraveling the signaling pathways promoting fibrosis in Dupuytren's disease reveals TNF as a therapeutic target. *Proc Natl Acad Sci U S A* **110**, E928-937, doi:10.1073/pnas.1301100110 (2013).

55 Eaton, C. in *Green's Operative Hand Surgery* Vol. 1 (eds SW Wolfe, WC Pederson, SH Kozin, & MS Cohen) Ch. 4: Dupuytren Disease, 148-181 (Elsevier, 2022).

56 Akbar, M. *et al.* Attenuation of Dupuytren's fibrosis via targeting of the STAT1 modulated IL-13Ralpha1 response. *Sci Adv* **6**, eaaz8272, doi:10.1126/sciadv.aaz8272 (2020).

57 Kida, H. *et al.* Dupuytren's contracture-associated SNPs increase SFRP4 expression in nonimmune cells including fibroblasts to enhance inflammation development. *Int Immunol*, doi:10.1093/intimm/dxad004 (2023).

58 Riesmeijer, S. A. *et al.* A genome-wide association meta-analysis implicates Hedgehog and Notch signaling in Dupuytren's disease. *Nat Commun* **15**, 199, doi:10.1038/s41467-023-44451-0 (2024).

59 Schultz, H. S. *et al.* Collagen induces maturation of human monocyte-derived dendritic cells by signaling through osteoclast-associated receptor. *J Immunol* **194**, 3169-3179, doi:10.4049/jimmunol.1402800 (2015).

60 Bakowska, J. C., Jupille, H., Fatheddin, P., Puertollano, R. & Blackstone, C. Troyer syndrome protein spartin is mono-ubiquitinated and functions in EGF receptor trafficking. *Mol Biol Cell* **18**, 1683-1692, doi:10.1091/mbc.e06-09-0833 (2007).

61 Augoff, K., Tabola, R., Kula, J., Gosk, J. & Rutowski, R. Epidermal growth factor receptor (EGF-R) in Dupuytren's disease. *J Hand Surg Br* **30**, 570-573, doi:10.1016/j.jhsb.2005.06.008 (2005).

62 Wilbrand, S. *Dupuytren's Contracture : Features and Consequences*, Acta Universitatis Upsaliensis, (2002).

63 Kuo, R. Y. L., Ng, M., Prieto-Alhambra, D. & Furniss, D. Dupuytren's Disease Predicts Increased All-Cause and Cancer-Specific Mortality: Analysis of a Large Cohort from the U.K. Clinical Practice Research Datalink. *Plast Reconstr Surg* **145**, 574e-582e, doi:10.1097/PRS.0000000000006551 (2020).

64 van Rijssen, A. L., ter Linden, H. & Werker, P. M. Five-year results of a randomized clinical trial on treatment in Dupuytren's disease: percutaneous needle fasciotomy versus limited fasciectomy. *Plast Reconstr Surg* **129**, 469-477, doi:10.1097/PRS.0b013e31823aea95 (2012).

65 Wilbrand, S., Ekbom, A. & Gerdin, B. The sex ratio and rate of reoperation for Dupuytren's contracture in men and women. *J Hand Surg Br* **24**, 456-459, doi:10.1054/jhsb.1999.0154 (1999).

66 Raykha, C. *et al.* IGF-II and IGFBP-6 regulate cellular contractility and proliferation in Dupuytren's disease. *Biochim Biophys Acta* **1832**, 1511-1519, doi:10.1016/j.bbadis.2013.04.018 (2013).

67 Hughes, C. S. *et al.* Single-pot, solid-phase-enhanced sample preparation for proteomics experiments. *Nat Protoc* **14**, 68-85, doi:10.1038/s41596-018-0082-x (2019).

68 Leutert, M., Rodriguez-Mias, R. A., Fukuda, N. K. & Villen, J. R2-P2 rapid-robotic phosphoproteomics enables multidimensional cell signaling studies. *Mol Syst Biol* **15**, e9021, doi:10.15252/msb.20199021 (2019).

69 Amodei, D. *et al.* Improving Precursor Selectivity in Data-Independent Acquisition Using Overlapping Windows. *J Am Soc Mass Spectrom* **30**, 669-684, doi:10.1007/s13361-018-2122-8 (2019).

70 Searle, B. C. *et al.* Chromatogram libraries improve peptide detection and quantification by data independent acquisition mass spectrometry. *Nat Commun* **9**, 5128, doi:10.1038/s41467-018-07454-w (2018).

71 Hoofnagle, A. N. *et al.* Multiple-reaction monitoring-mass spectrometric assays can accurately measure the relative protein abundance in complex mixtures. *Clin Chem* **58**, 777-781, doi:10.1373/clinchem.2011.173856 (2012).

72 Gold, L. *et al.* Aptamer-based multiplexed proteomic technology for biomarker discovery. *PLoS One* **5**, e15004, doi:10.1371/journal.pone.0015004 (2010).

73 Berrone, E. *et al.* SOMAscan Proteomics Identifies Novel Plasma Proteins in Amyotrophic Lateral Sclerosis Patients. *Int J Mol Sci* **24**, doi:10.3390/ijms24031899 (2023).

74 Network, T. C. R. A. *gee: Generalized Estimation Equation Solver*, <https://cran.r-project.org/package=gee> (2023).

75 Kuhn, M. Building Predictive Models in R Using the caret Package. *Journal of Statistical Software* **28** (2008).

Acknowledgments

This work was funded entirely by the Dupuytren Research Group, a 501 (c) (3) nonprofit organization.

Gail Solomon assisted with manuscript writing.

PS, AL, AG: recipients of grant UM1TR004398 (the Tufts NIH CTSA award).

Databank and study support from FORWARD, the National Databank for Rheumatic Diseases, is gratefully acknowledged.

Author Contributions

CE provided the study design and wrote the main manuscript text. CE and BH wrote the results section, and BS and PS wrote the methods section. All authors performed data analysis.

Data Availability

All the data and analytic scripts that support the findings of this study are openly available in the Github repository Dup_Blood_Proteomic_Data at https://github.com/Dupuytren/Dup_Blood_Proteomic_Data.

Competing Interest Statement

These authors declare the following competing interests: Morten Karsdal, Cecilie Bager, and Signe Holm Nielsen are all currently employed by Nordic Bioscience; Morten Karsdal, Cecilie Bager, and Signe Holm Nielsen hold stocks in Nordic Bioscience. The rest of the authors have no conflicts of interest to declare.

Figure sources

Figure 1. Each panel image was generated in R https://www.r-project.org. The final image was assembled and annotated with Moho 13.5.5 https://moho.lostmarble.com.

Figure 2. The image was generated in R https://www.r-project.org.

Figure 3. Panels a and b were generated in R https://www.r-project.org. Panel C was downloaded from STRING https://string-db.org. The final image was assembled and annotated with Moho 13.5.5 https://moho.lostmarble.com.

Figure 4. Panels a and b were generated in R https://www.r-project.org. Panel C was downloaded from STRING https://string-db.org. The final image was assembled and annotated with Moho 13.5.5 https://moho.lostmarble.com.

Supplementary Fig. S1 online was created in PowerPoint.

Supplementary Fig. S2 online was created in Excel.

Supplementary Fig. S3 online was created in Excel.

Supplementary Fig. S4 online was generated in R https://www.r-project.org.

Supplementary Fig. S5 online was generated in R https://www.r-project.org.

Figure Legends

Figure 1. Differential production of Dupuytren vs. control collagen metabolism markers. A) Collagen I degradation marker C1M. B) Collagen I synthesis to degradation marker ratio Pro-C1/C1M. C) Collagen V synthesis marker Pro-C5. D) Collagen VII synthesis marker Pro-C7. * p-value <0.05, **p-value <0.005.

Figure 2. Heatmap of log-transformed standardized values of the 54 significant proteins in the hypothesis-free analysis.

Figure 3. Hypothesis-Free DPRS and Protein-protein interactions. A) The Hypothesis-free Diagnostic Proteomic Risk Score has an AUC-ROC value of 0.8. B) Hypothesis-free Diagnostic Proteomic Risk Scores (HF-DPRS) of the control vs Dupuytren cohorts. p-value = 5.28E-06. C) Network expression of 54 differentially expressed proteins. Of the 54 proteins, 30 had strong pathway connections in the network: ACAN, AKR1A1, C5, C6, CALCB, CASP3, CGA, CGB3, CPB1, CRKL, DSG2, EIF4H, FKBP5, G3BP2, GP1BB, GUSB, HGS, HSP90AA1, KNG1, MAP3K11, MBNL1, MBNL2, NRG4, OSCAR, PCSK9, POSTN, PRSS1, SERPINC1, SOCS3, SYK, TF, USP8, and YWHAB.

Figure 4. Hypothesis-based DPRS and Protein-protein interactions. A) The Hypothesis-based Diagnostic Proteomic Risk Score has an AUC-ROC value of 0.9. AUC-ROC (Area Under the

Curve - Receiver Operating Characteristics) is an index of predictive accuracy. B) Hypothesis-free Diagnostic Proteomic Risk Scores (HF-DPRS) of the control vs Dupuytren cohorts. (p-value = 7.79E-09). C) Network expression of 23 differentially expressed proteins. Of the 23 proteins, 20 had strong pathway connections: DAB2, SMAD1, USP8, PLAT, SFRP4, ACAN, DDR2, HPX, KNG1, LCN2, SERPINH1, TF, MAP2K1, PRKCA, STAT1, YWHAZ, POSTN, COL1A1, CASP3, and STAT3.

Figure 1.

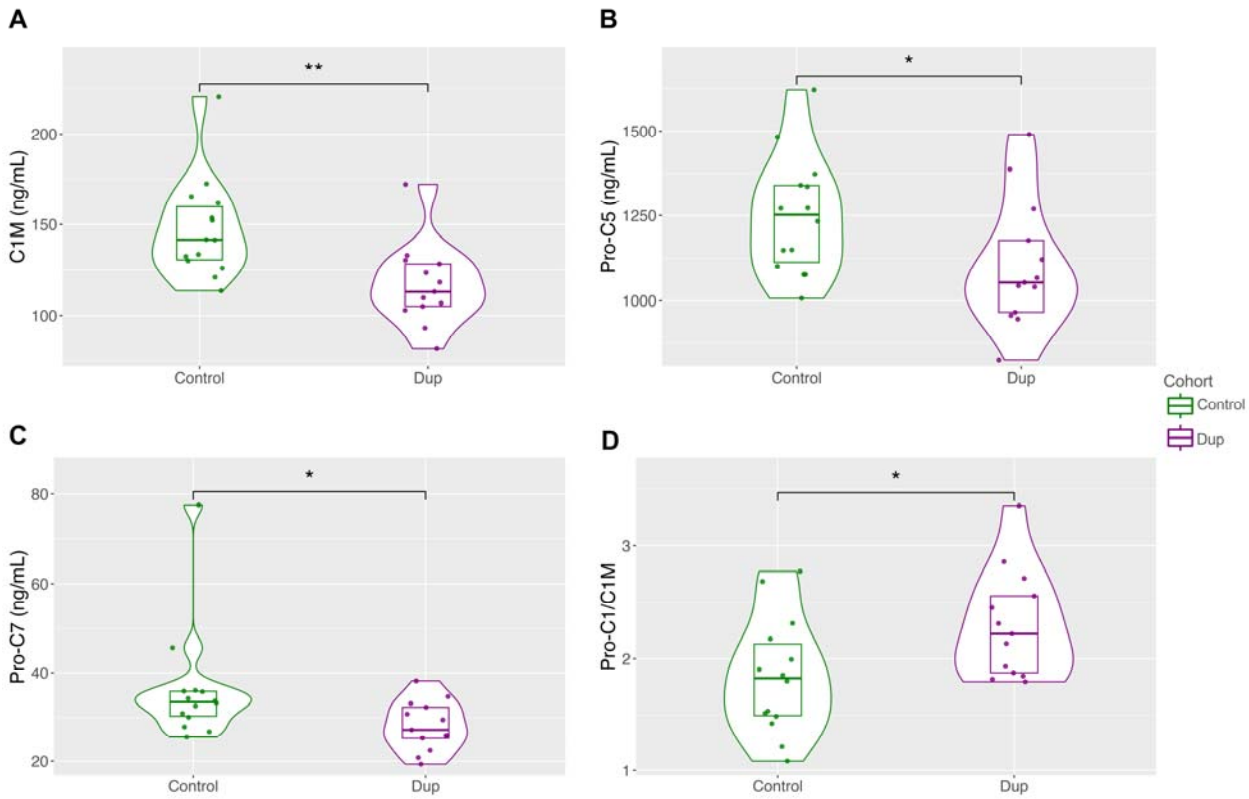
A
**
C1M (ng/mL)
200
150
100
Control
Dup
B
*
Pro-C5 (ng/mL)
1500
1250
1000
Control
Dup
Cohort
Control
Dup
C
*
Pro-C7 (ng/mL)
80
60
40
20
Control
Dup
D
*
Pro-C1/C1M
3
2
1
Control
Dup

Figure 2.

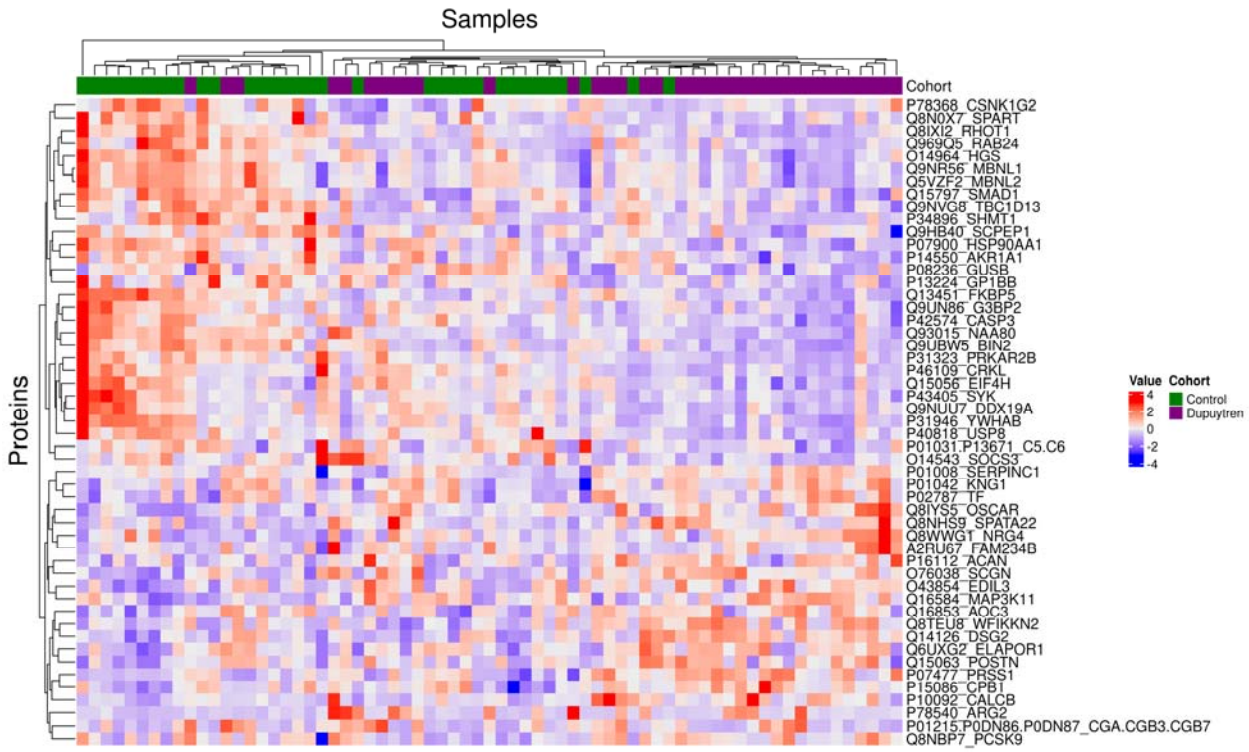
Samples
Cohort
Proteins
P78368_CSNK1G2
Q8N0X7_SPART
Q8IXI2_RHOT1
Q969Q5_RAB24
O14964_HGS
Q9NR56_MBNL1
Q5VZF2_MBNL2
Q15797_SMAD1
Q9NVG8_TBC1D13
P34896_SHMT1
Q9HB40_SCPEP1
P07900_HSP90AA1
P14550_AKR1A1
P08236_GUSB
P13224_GP1BB
Q13451_FKBP5
Q9UN86_G3BP2
P42574_CASP3
Q93015_NAA80
Q9UBW5_BIN2
P31323_PRKAR2B
P46109_CRKL
Q15056_EIF4H
P43405_SYK
Q9NUU7_DDX19A
P31946_YWHAB
P40818_USP8
P01031;P13671_C5;C6
O14543_SOCS3
P01008_SERPINC1
P01042_KNG1
P02787_TF
Q8IYS5_OSCAR
Q8NHS9_SPATA22
Q8WWG1_NRG4
A2RU67_FAM234B
P16112_ACAN
Q76038_SCGN
O43854_EDIL3
Q16584_MAP3K11
Q16853_AOC3
Q8TEU8_WFIKKN2
Q14126_DSG2
Q6UXG2_ELAPOR1
Q15063_POSTN
P07477_PRSS1
P15086_CPB1
P10092_CALCB
P78540_ARG2
P01215;P0DN86;P0DN87_CGA;CGB3;CGB7
Q8NBP7_PCSK9
Value
4
2
0
-2
-4
Cohort
Control
Dupuytren

Figure 3.

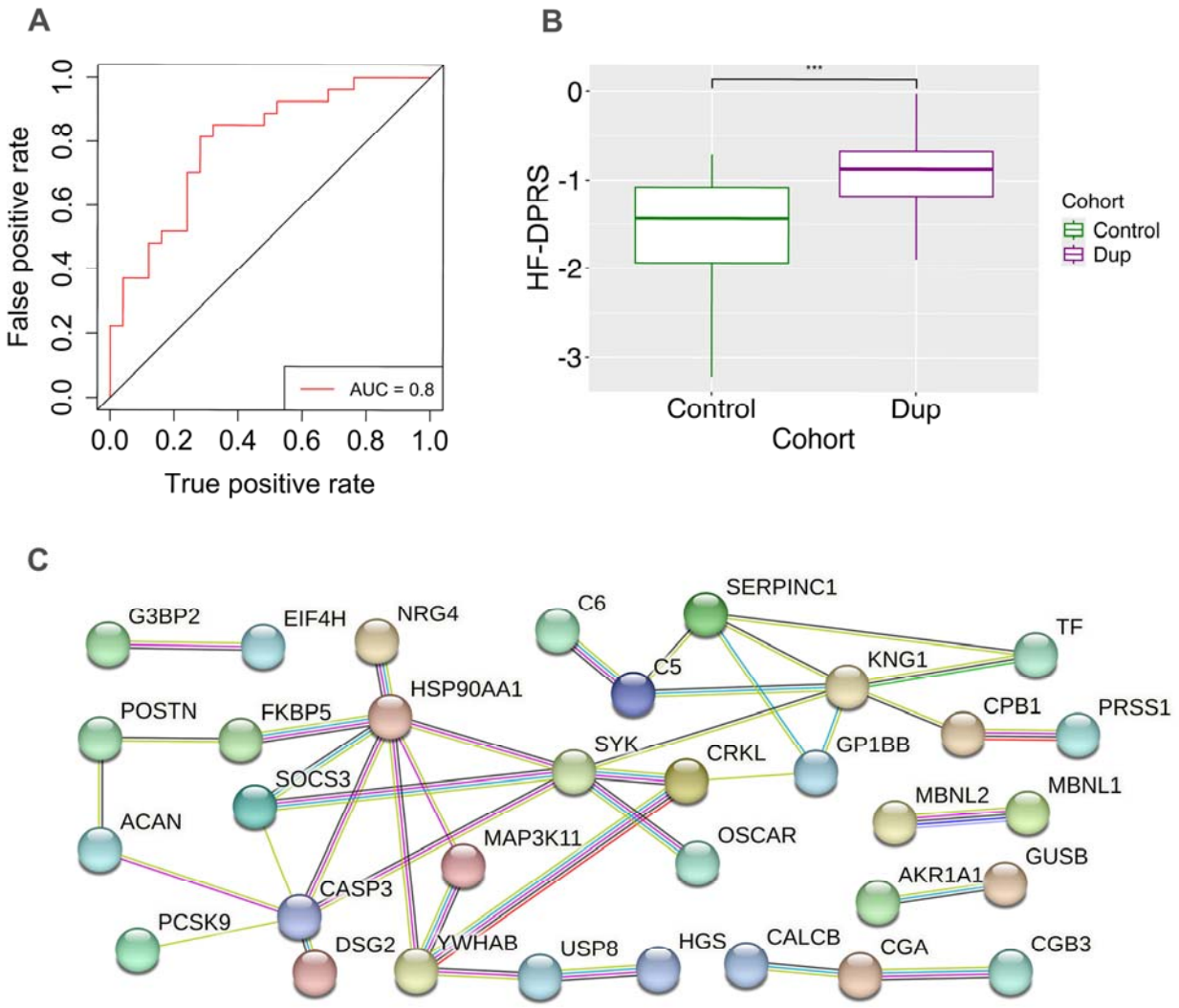
A
False positive rate
True positive rate
AUC = 0.8
B
HF-DPRS
Cohort
Control
Dup
C
G3BP2
EIF4H
NRG4
C6
SERPINC1
TF
C5
KNG1
HSP90AA1
POSTN
FKBP5
CPB1
PRSS1
SYK
CRKL
GP1BB
SOCS3
MBNL2
MBNL1
ACAN
MAP3K11
OSCAR
GUSB
AKR1A1
CASP3
PCSK9
DSG2
YWHAB
USP8
HGS
CALCB
CGA
CGB3

Figure 4.

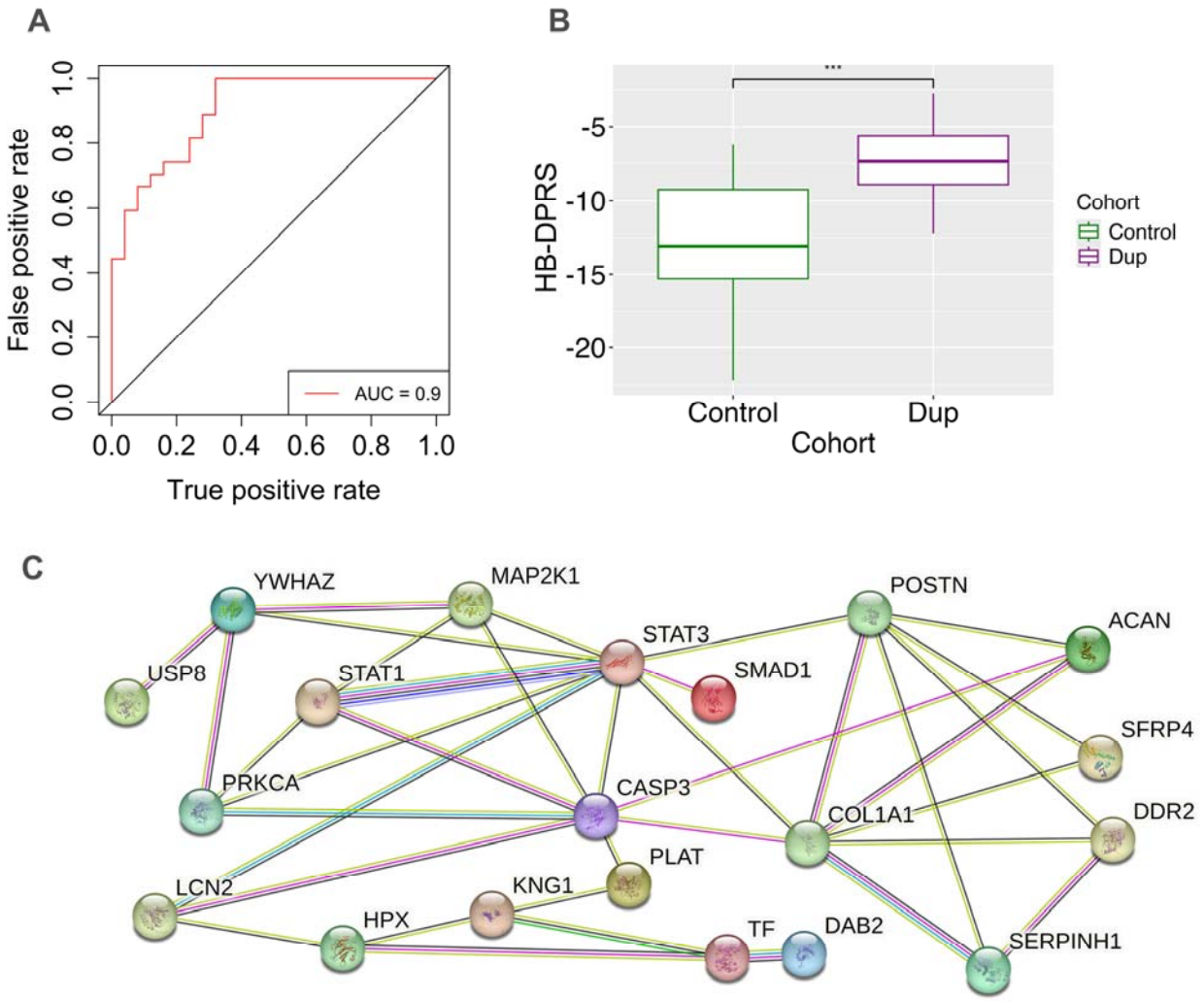
A
False positive rate
True positive rate
0.0
0.2
0.4
0.6
0.8
1.0
AUC = 0.9
B
HB-DPRS
-5
-10
-15
-20
***
Control
Dup
Cohort
Cohort
Control
Dup
C
YWHAZ
MAP2K1
POSTN
ACAN
STAT3
USP8
STAT1
SMAD1
SFRP4
PRKCA
CASP3
COL1A1
DDR2
PLAT
LCN2
KNG1
HPX
TF
DAB2
SERPINH1

Table 1. Collagen epitope markers and findings

Assay	D/C	Description	Represents	p-value	SE	FC (D/C)
PRO_C1_HP	ns	Internal epitope in the N-terminal propeptide of type I collagen	Col I Synthesis	0.9437	C 10.99 D 11.89	0.93
C1M_HP	Down**	MMP generated fragment of the a1 chain of type I collagen	Col I Degradation	0.0036	C 5.25 D 4.30	0.73
PRO-C2_HP	ns	N-terminal fragment of type IIB procollagen	Col II Synthesis	0.7808	C 1.45 D 3.11	1.01
CALC2	ND	C-terminal propeptide of type II collagen	Col II Synthesis	NA	NA	NA
C2M_HP	ns	MMP generated fragment of type II collagen	Col II Degradation	0.1607	C 1.52 D 1.16	1.29
PRO-C3_roHP	ns	N-terminal propeptide of type III collagen	Col III Synthesis	0.9951	C 1.04 D 1.24	0.93
C3M_HP	ns	MMP-9 generated fragments of type III collagen	Col III Degradation	0.1615	C 16.96 D 13.61	0.86
CTX-III_HP	ns	MMP generated fragment of crosslinked type III collagen	Col III Degradation	0.4887	C 40.88 D 53.26	0.91
PRO-C4_HP	ns	Internal epitope in the 7S domain of type IV collagen	Col IV Synthesis	0.0739	C 195.98 D 183.12	0.84
C4M_HP	ns	MMP generated fragment of the a1 chain of type IV collagen	Col IV Degradation	0.1014	C 8.89 D 7.42	0.84
PRO-C5_HP	Down*	C-terminal propeptide of type V collagen	Col V Synthesis	0.0458	C 33.17 D 35.88	0.82
PRO-C6_roHP	ns	C-terminal propeptide of type VI collagen alpha-3 chain	Col VI Synthesis	0.7222	C 0.27 D 0.27	0.92
C6M_HP	ns	MMP2 generated fragment of type VI collagen	Col VI Degradation	0.1097	C 22.31 D 23.41	0.83
PRO_C7 HP	Down*	BMP-I mediated neo-epitope in the NC-2 propeptide of type Vll collagen	Col VII Synthesis	0.0480	C 2.49 D 1.08	0.72
C7M	ND	Neo-epitope of MMP13 degradation of type Vll collagen	Col VII Degradation	NA	NA	NA
PRO-C9	ns	C-terminus of NC-I domain of the a1 chain of type IX collagen	Col IX Synthesis	0.9658	C 0.80 D 0.65	0.92

Synthesis and degradation markers of Collagen I, II, III, IV, V, VII, and IX. Compared to controls, there were significant reductions in markers of Collagen I degradation, Collagen V synthesis, and Collagen VII synthesis. D/C: ratio of Dupuytren to control values. FC: fold change. **: <0.005, *: <0.05. ns: not significant. ND: undetectable in both disease and control cohorts.

Table 2. Hypothesis-free Diagnostic Proteomic Risk Score

Protein	Eff	SE	p-value	FDR
Spartin	-11.62125	2.97479	0.000094	0.18
Oscar	13.99037	3.596067	0.0001	0.18

Proteins of the Hypothesis-free DPRS. Eff = log (odds ratio comparing Dup to control) for a change of 1 in the log (protein data). SE: Standard error. FDR: False Discovery Rate (Adjusted p-value).

Table 3. Hypothesis-based Diagnostic Proteomic Risk Score

Protein	Eff	SE	p-value	FDR
SMAD1*	-6.3649	1.877804	0.0007	0.12
CSMD1	5.397535	1.907423	0.00466	0.18
SH3BP2	-4.59151	1.582341	0.00371	0.18
POSTN*	4.305245	1.502627	0.00417	0.18
ACAN*	5.589134	1.75746	0.00147	0.12
LCN2	-4.73895	1.734879	0.0063	0.19
AOC3*	7.050175	2.62144	0.00716	0.2
DDR2	1.63418	0.595212	0.00604	0.19
USP8*	-3.30095	1.041269	0.00152	0.12
CSNK1G2*	-10.3331	3.593633	0.00404	0.18
SERPINH1	-2.6813	0.799538	0.0008	0.12

Proteins of the Hypothesis-based DPRS. Eff = log (odds ratio comparing Dup to control) for a change of 1 in the log (protein data). SE: Standard error. FDR: False Discovery Rate (Adjusted p-value). * Five also had significant differential expression in the 54 proteins identified in the hypothesis-free analysis.

Table 4. Mass Spectrometry (MS) – SomaScan (SS) concordance

Protein	Est MS	p-val MS	FDR MS	Est SS	p-val SS	FDR SS
AOC3	0.214854	0.076413	0.232677	0.116624	0.000845	0.217972
POSTN	0.410212	0.098842	0.232677	0.182892	0.000312	0.211479
SERPINC1	0.071331	0.116338	0.232677	0.091474	0.001500	0.225251
TF	0.035200	0.567393	0.829196	0.076715	0.000025	0.172072
PCSK9	0.165811	0.755318	0.829196	0.185675	0.001371	0.222267
KNG1	0.010065	0.829196	0.829196	0.065561	0.000490	0.217972

Six proteins identified by MS were also in the 54 proteins found in the hypothesis-free SS analysis. AOC3, POSTN, SERPINC1, TF, PCSK9, and KNG1. Of these, AOC3, POSTN, and SERPINC1 had False Discovery Rate (FDR, Adjusted p-value) <0.25 in both Mass Spec and SomaLogic analyses.

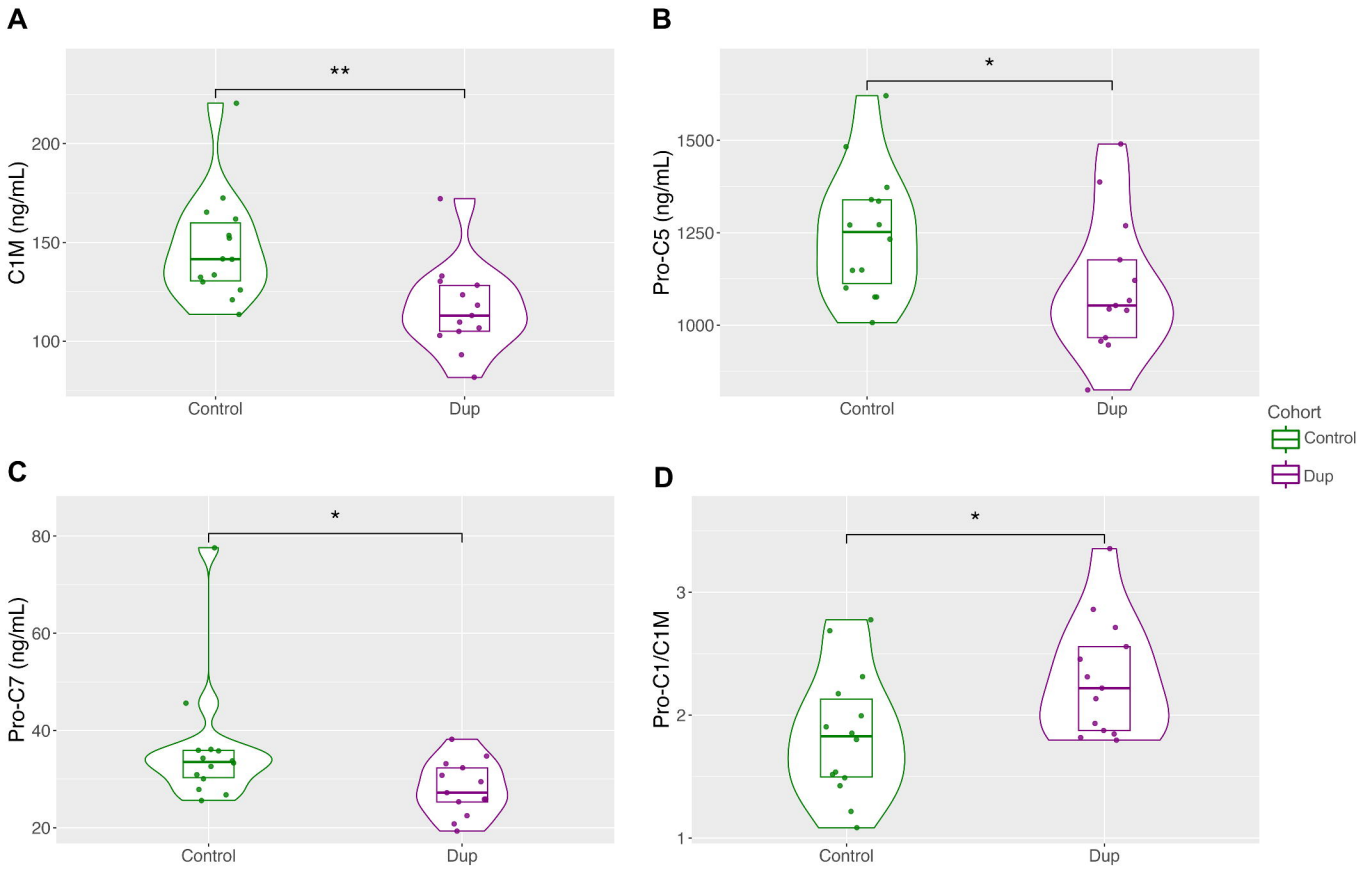
A
**
C1M (ng/mL)
200
150
100
Control
Dup
B
*
Pro-C5 (ng/mL)
1500
1250
1000
Control
Dup
Cohort
Control
Dup
C
*
Pro-C7 (ng/mL)
80
60
40
20
Control
Dup
D
*
Pro-C1/C1M
3
2
1
Control
Dup

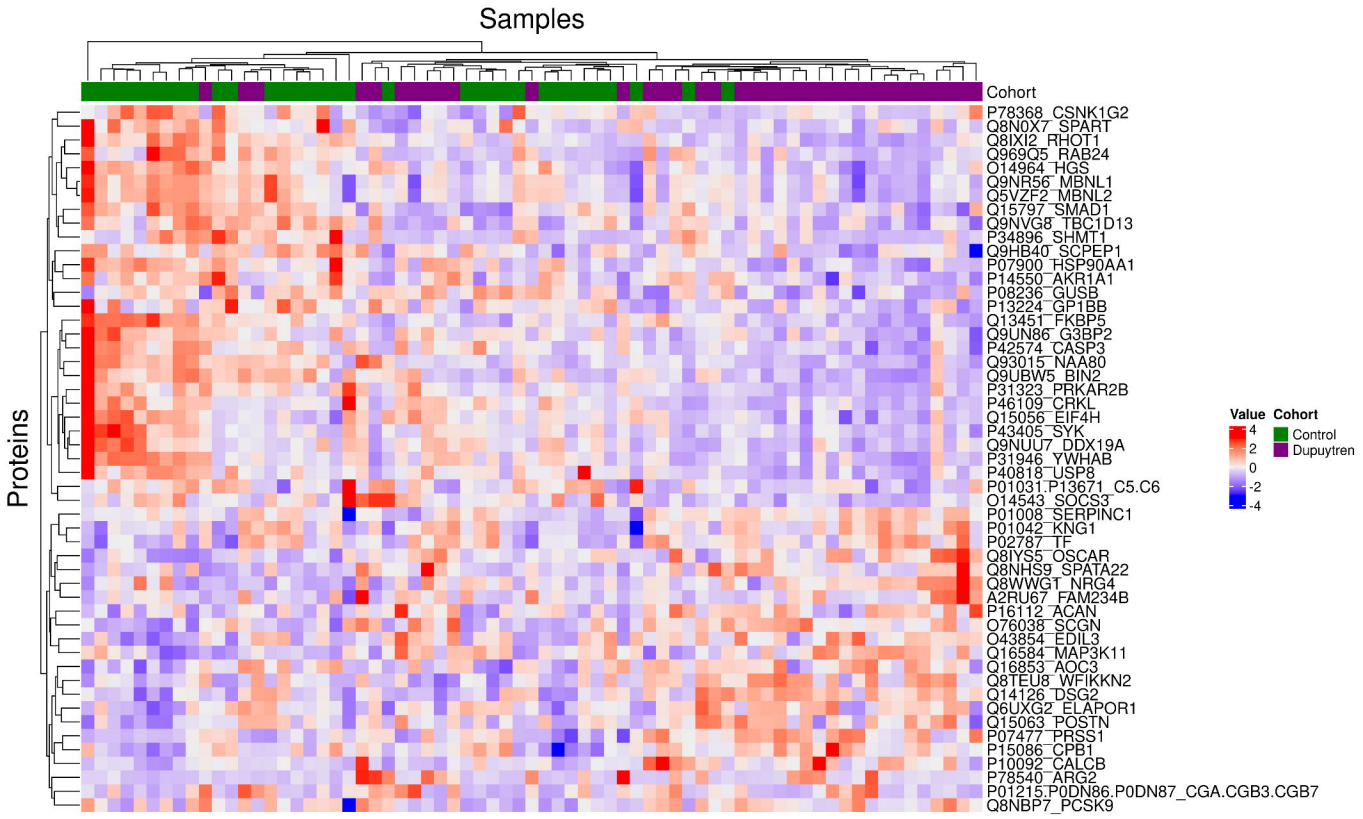
Samples
Cohort
Proteins
P78368_CSNK1G2
Q8N0X7_SPART
Q8IXI2_RHOT1
Q969G5_RAB24
O14964_HGS
Q9NR56_MBNL1
Q5VZF2_MBNL2
Q15797_SMAD1
Q9NVG8_TBC1D13
P34896_SHMT1
Q9HB40_SCPEP1
P07900_HSP90AA1
P14550_AKR1A1
P08236_GUSB
P13224_GP1BB
Q13451_FKBP5
Q9UN86_G3BP2
P42574_CASP3
Q93015_NAA80
Q9UBW5_BIN2
P31323_PRKAR2B
P46109_CRKL
Q15056_EIF4H
P43405_SYK
Q9NUU7_DDX19A
P31946_YWHAB
P40818_USP8
P01031.P13671_C5.C6
O14543_SOCS3
P01008_SERPINC1
P01042_KNG1
P02787_TF
Q8IYS5_OSCAR
Q8NHS9_SPATA22
Q8WWG1_NRG4
A2RU67_FAM234B
P16112_ACAN
O76038_SCGN
O43854_EDIL3
Q16584_MAP3K11
Q16853_AOC3
Q8TEU8_WFIKKN2
Q14126_DSG2
Q6UXG2_ELAPOR1
Q15063_POSTN
P07477_PRSS1
P15086_CPB1
P10092_CALCB
P78540_ARG2
P01215.P0DN86.P0DN87_CGA.CGB3.CGB7
Q8NBP7_PCSK9
Value
4
2
0
-2
-4
Cohort
Control
Dupuytren

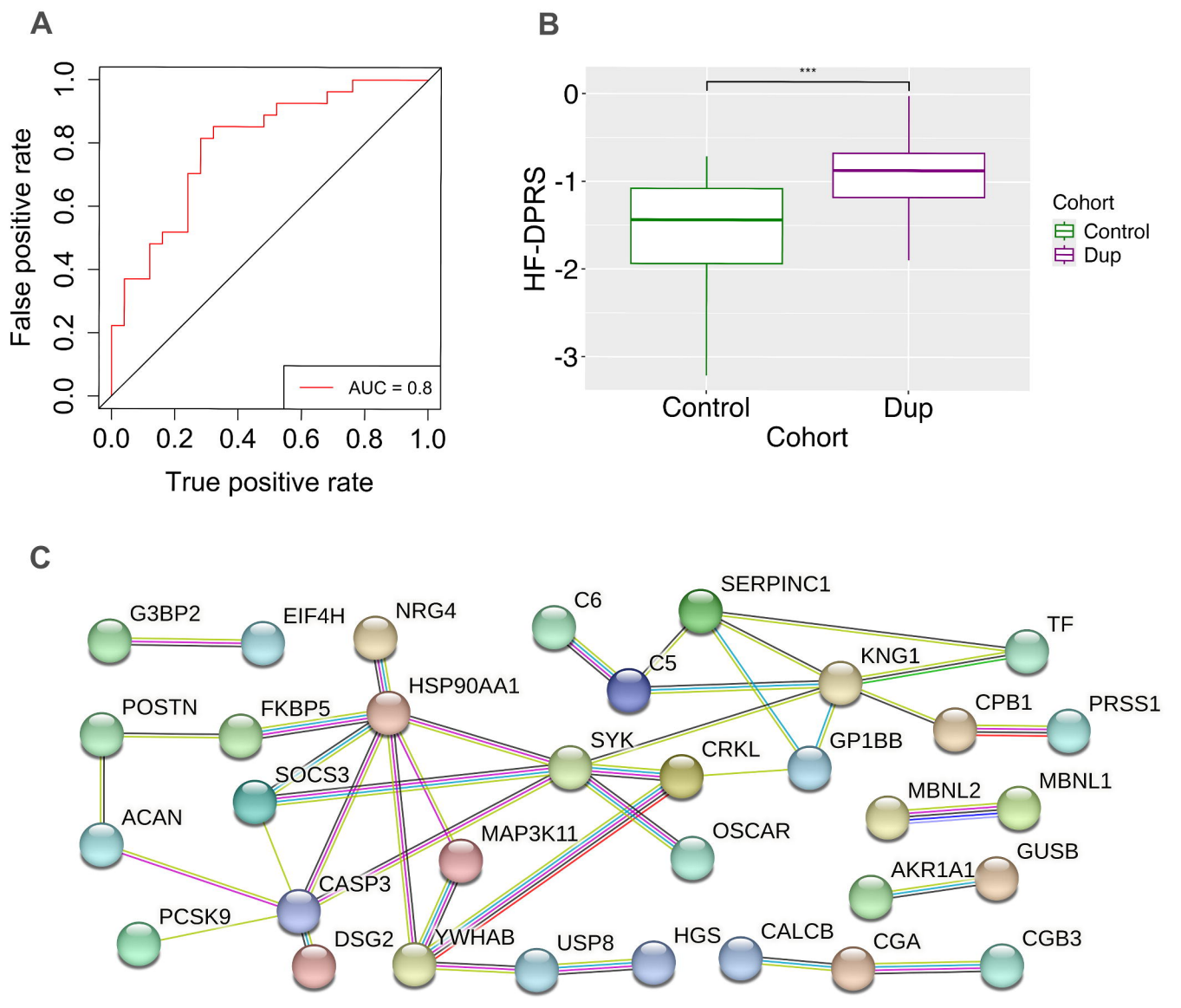
A
False positive rate
True positive rate
0.0
0.2
0.4
0.6
0.8
1.0
AUC = 0.8
B
HF-DPRS
0
-1
-2
-3
***
Control
Dup
Cohort
Cohort
Control
Dup
C
G3BP2
EIF4H
NRG4
C6
SERPINC1
TF
C5
KNG1
HSP90AA1
POSTN
FKBP5
CPB1
PRSS1
SYK
CRKL
GP1BB
SOCS3
MBNL2
MBNL1
ACAN
MAP3K11
OSCAR
GUSB
AKR1A1
CASP3
PCSK9
DSG2
YWHAB
USP8
HGS
CALCB
CGA
CGB3

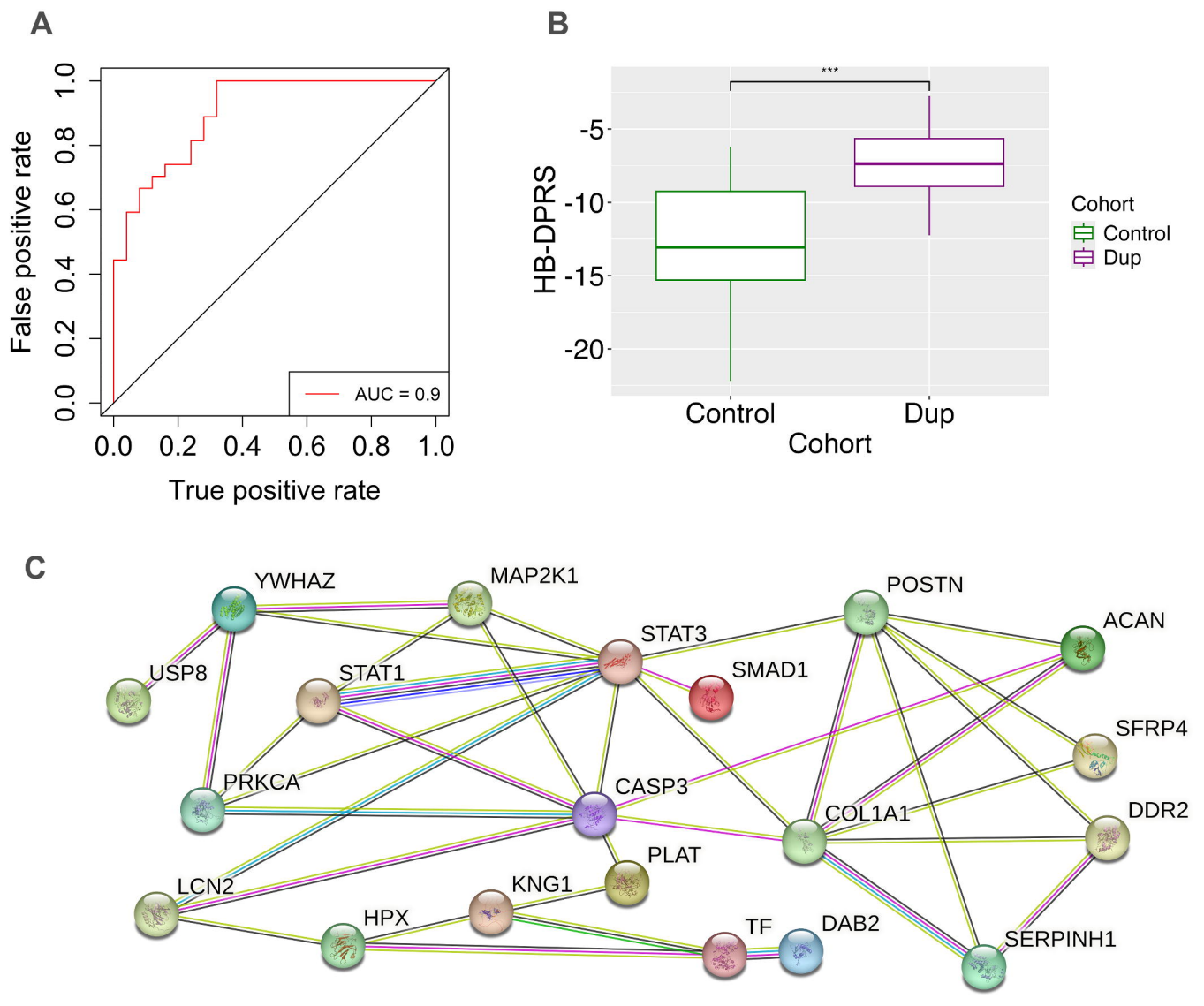
A
False positive rate
True positive rate
0.0
0.2
0.4
0.6
0.8
1.0
AUC = 0.9
B
HB-DPRS
-5
-10
-15
-20
***
Control
Dup
Cohort
Cohort
Control
Dup
C
YWHAZ
MAP2K1
POSTN
ACAN
STAT3
USP8
STAT1
SMAD1
SFRP4
PRKCA
CASP3
COL1A1
DDR2
PLAT
LCN2
KNG1
HPX
TF
DAB2
SERPINH1

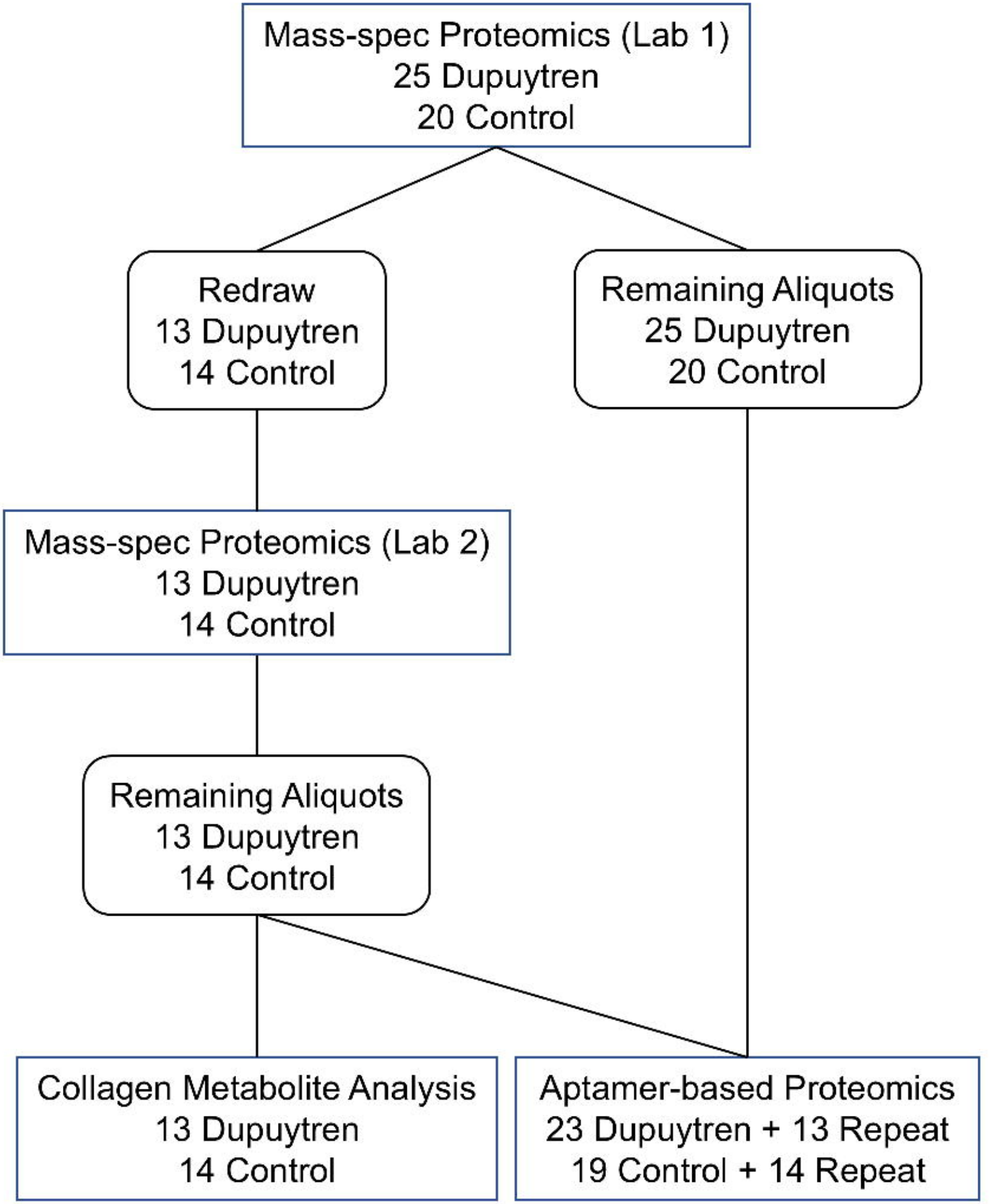
Mass-spec Proteomics (Lab 1)
25 Dupuytren
20 Control
Redraw
13 Dupuytren
14 Control
Remaining Aliquots
25 Dupuytren
20 Control
Mass-spec Proteomics (Lab 2)
13 Dupuytren
14 Control
Remaining Aliquots
13 Dupuytren
14 Control
Collagen Metabolite Analysis
13 Dupuytren
14 Control
Aptamer-based Proteomics
23 Dupuytren + 13 Repeat
19 Control + 14 Repeat

	C&C	ECM	ENZ	MBR	PPL	SGN
ACAN		■				
AKR1A1		■				
BIN2		■				
C5	■	■	■			■
C6	■	■				
CALCB		■				■
CASP3			■			■
CGA		■				■
CGB3		■				
CGB7		■				
CPB1		■				
CRKL				■	■	■
CSNK1G2						■
DSG2		■				■
EDIL3		■				
FKBP5		■				■
GUSB		■				
HGS		■				■
HSP90AA1						■
KNG1	■		■			■
MAP3K11						■
NRG4						■
PCSK9				■		
PRKAR2B			■			■
RHOT1						■
SERPINC1	■		■			
SOCS3			■		■	
SYK				■	■	
TF				■		
USP8				■		
WFIKKN2			■			
YWHAB			■		■	

	CAN	C&C	ECM	INL	INF	MBR	MFB	PPL	SGN	WNT
ACAN			■							
CASP3	■		■	■	■		■	■	■	
COL1A1	■	■	■		■	■	■	■	■	■
CSNK1G2								■		■
DAB2							■	■		■
DDR2			■			■	■	■		
HPX			■					■	■	
KNG1	■	■	■		■		■			
LCN2				■						
MAP2K1	■		■	■	■	■	■	■	■	
PLAT	■	■					■	■	■	
POSTN			■							
PRKCA	■	■	■		■	■	■	■	■	■
SERPINH1			■							
SFRP4							■			■
SMAD1							■	■		
STAT1	■		■	■	■	■	■	■	■	
STAT3	■		■	■	■	■	■	■	■	
TF	■	■					■	■		
USP8							■	■		■
YWHAZ	■	■		■	■		■	■		■

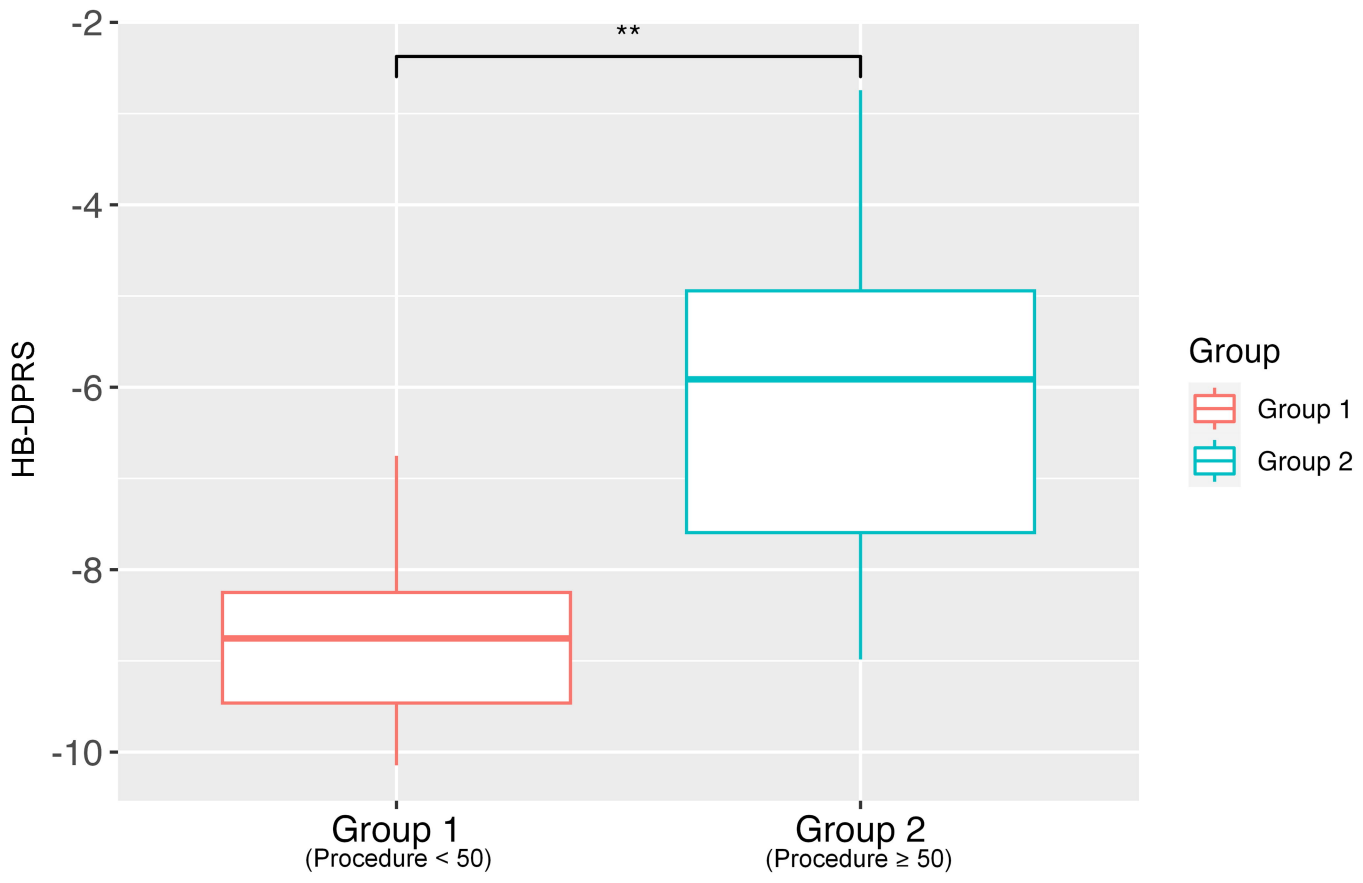
**
-2
-4
-6
-8
-10
HB-DPRS
Group 1
(Procedure < 50)
Group 2
(Procedure ≥ 50)
Group
Group 1
Group 2

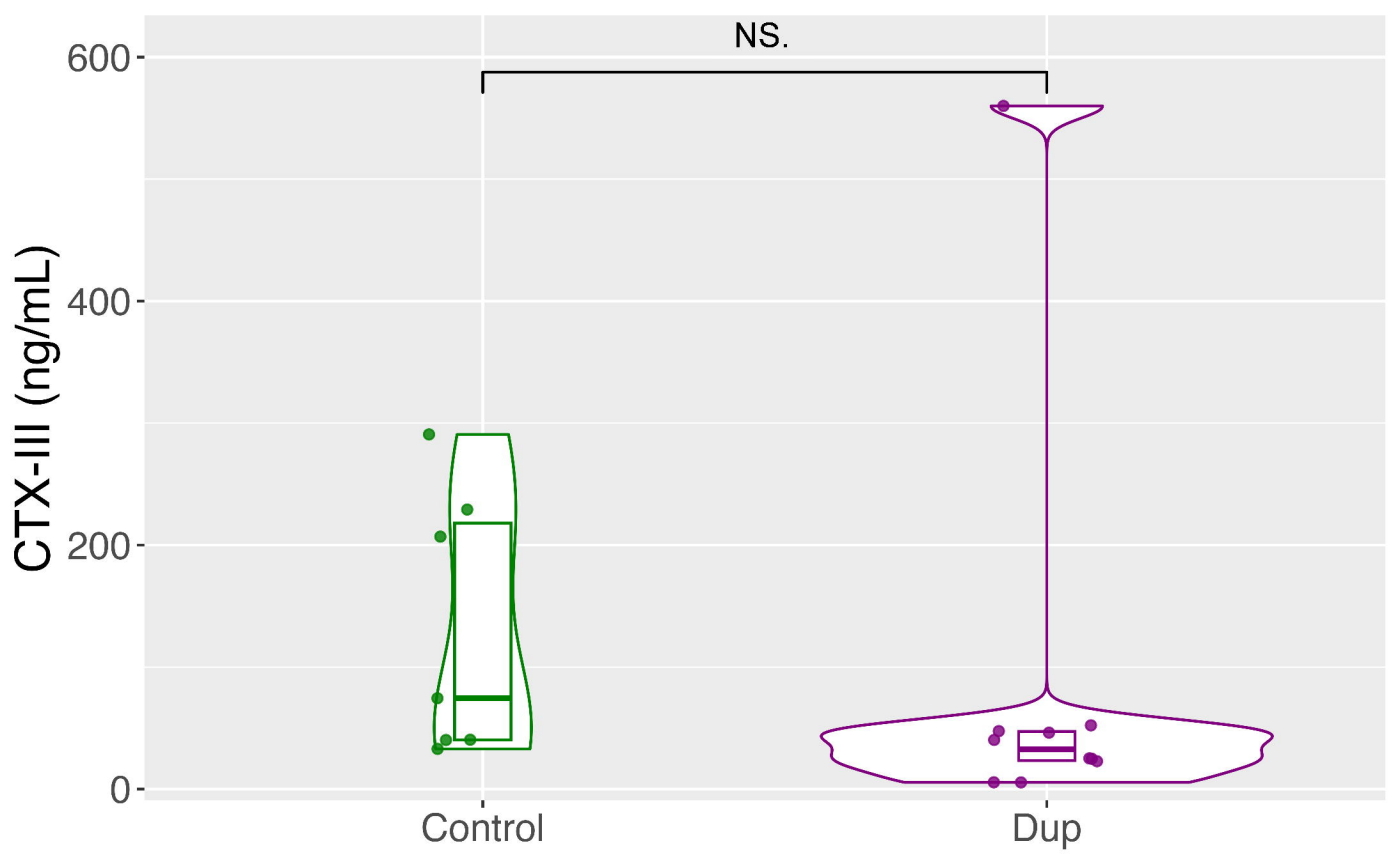
NS.
600
400
200
0
CTX-III (ng/mL)
Control
Dup